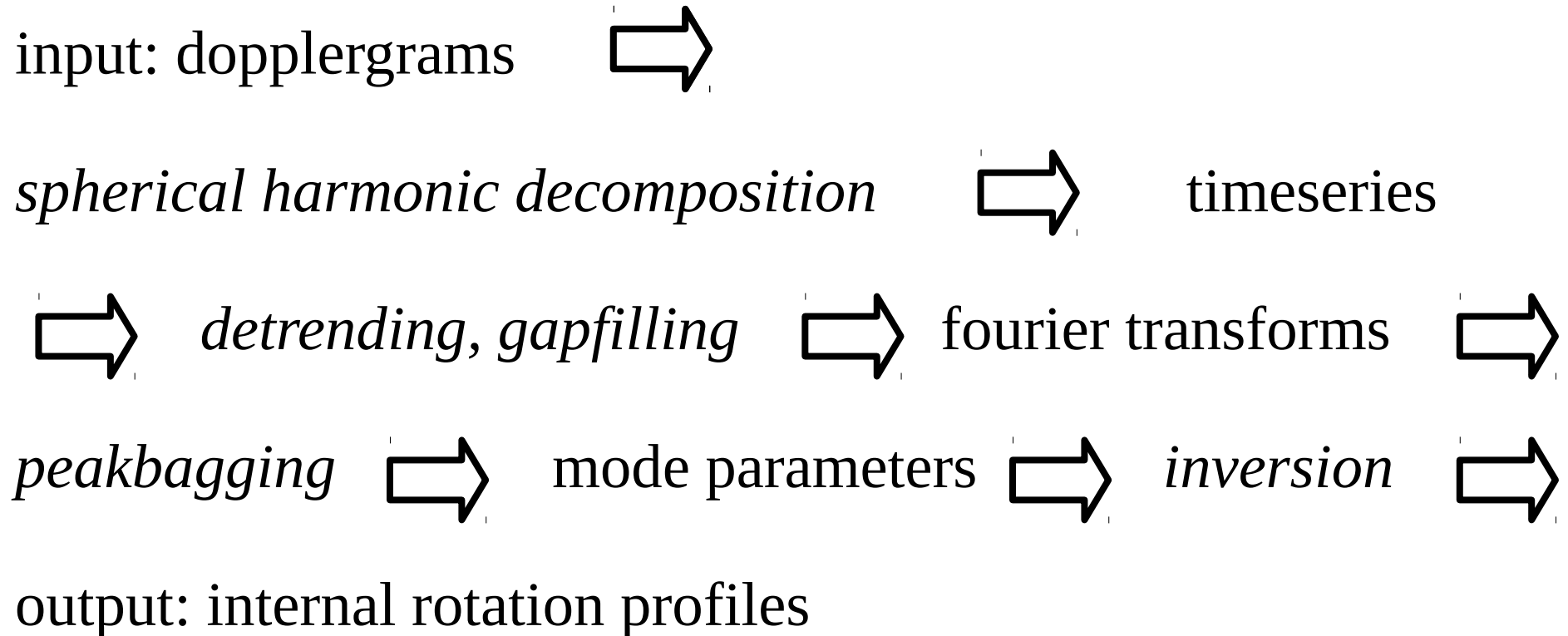


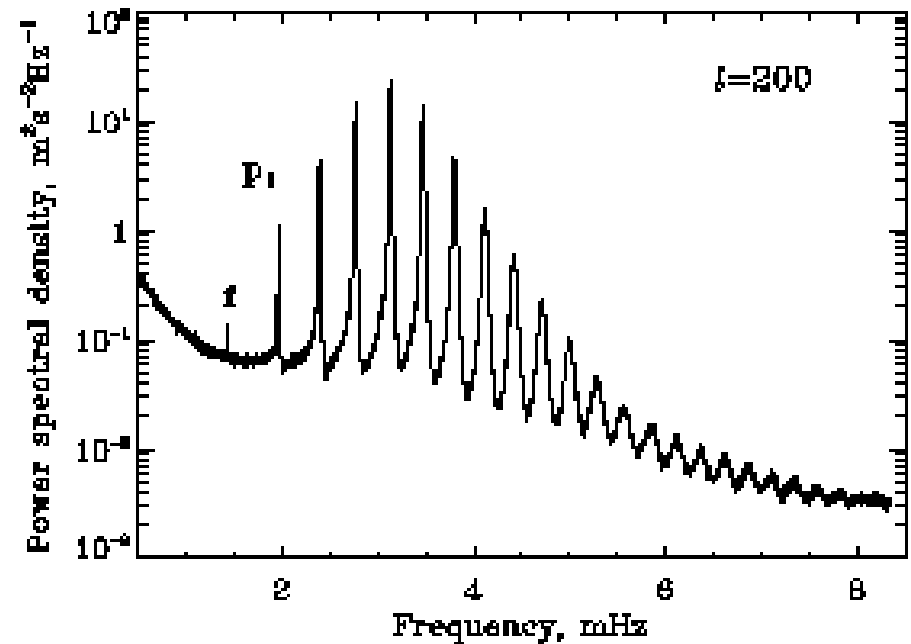
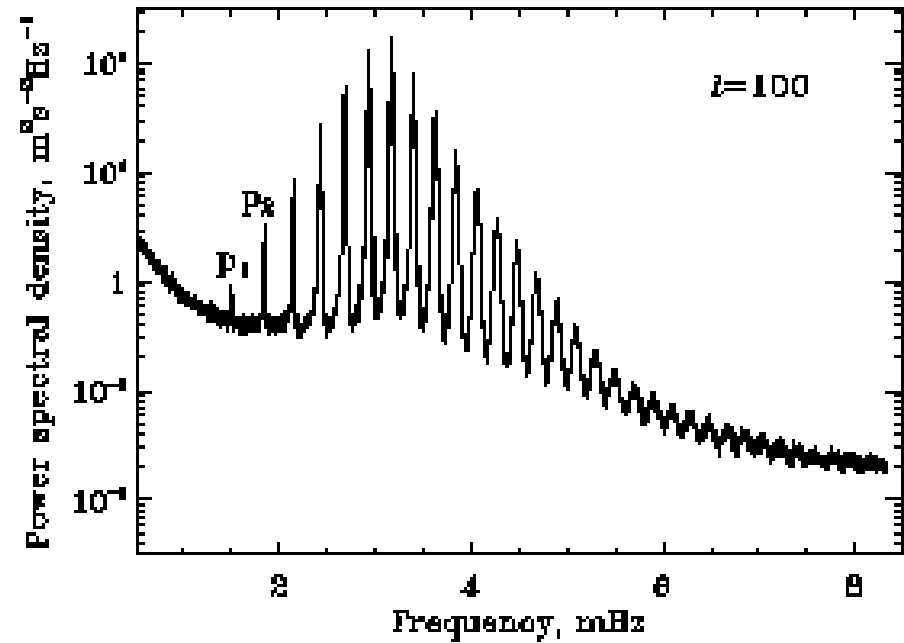
Global-Mode Helioseismology with MDI and HMI: Problems and Progress

tim larson
tplarson@sun.stanford.edu

Dataflow Overview



Example: Power Spectra



Peakbagging

Fourier components normally distributed. Variance caused by a single mode at frequency ν :

$$v(\nu_0, w, A, \nu) = \frac{2wA^2}{w^2 + 4(\nu - \nu_0)^2}$$

ν_0 = peak frequency, A = amplitude, w = width

Maximum Likelihood

Maximize joint probability of a given mode, which is given by the product of probability densities over a suitable number of frequency bins.

Equivalent to minimizing the negative logarithm:

$$S(\nu_0, w, A) = \sum_i \ln (v(\nu_i)) + \frac{x(\nu_i)^2 + y(\nu_i)^2}{v(\nu_i)}.$$

Where x and y are the real and imaginary parts of the fourier transform.

Frequency splitting

Rather than fit all modes separately, fit all values of m simultaneously. Frequency given by a sum over polynomials:

$$\nu_{n\ell m} = \nu_0(n, \ell) + \sum_{i=1}^{N_a} a_i(n, \ell) \mathcal{P}_i^\ell(m)$$

Redefine ν_0 as mean multiplet frequency for a given n and ℓ , and fit for a_i directly. Amplitude and width presumed the same for all m .

Leakage Matrix

Observed timeseries is given by a superposition of modes on the Sun:

$$o_{\ell m}(t) = \sum_{n' \ell' m'} c_{\ell m, \ell' m'}^{RR} \operatorname{Re}[a_{n' \ell' m'}(t)] + i c_{\ell m, \ell' m'}^{II} \operatorname{Im}[a_{n' \ell' m'}(t)]$$

or in frequency space:

$$\tilde{o}_{\ell m}(\nu) = x_{\ell m}(\nu) + iy_{\ell m}(\nu) = \sum_{n' \ell' m'} C_{\ell m, \ell' m'} \tilde{a}_{n' \ell' m'}(\nu)$$

where

$$C = (c^{RR} + c^{II})/2$$

Covariance

$$\begin{aligned} E_{\ell m, \ell' m'}^{\text{modes}}(\nu_i) &= \text{Cov}[x_{\ell m}(\nu_i), x_{\ell' m'}(\nu_i)] = \text{Cov}[y_{\ell m}(\nu_i), y_{\ell' m'}(\nu_i)] \\ &= \sum_{n'' \ell'' m''} C_{\ell m, \ell'' m''} C_{\ell' m', \ell'' m''} v_{n'' \ell'' m''}(\mathbf{p}, \nu_i). \end{aligned}$$

Fit one value of l at a time. Total covariance used:

$$E_{m, m'}(\nu_i) = E_{m, m'}^{\text{modes}}(\nu_i) + \tilde{E}_{m, m'} \frac{\nu_B}{\nu_i} e^b$$

Second term includes measured covariance at high frequency. ν_B is a constant, fit for b .

Mode Parameters

function to minimize now becomes

$$S(\mathbf{p}) = \sum_i \ln |\mathbf{E}(\mathbf{p}, \nu_i)| + \mathbf{x}(\nu_i)^T \mathbf{E}(\mathbf{p}, \nu_i) \mathbf{x}(\nu_i) + \mathbf{y}(\nu_i)^T \mathbf{E}(\mathbf{p}, \nu_i) \mathbf{y}(\nu_i)$$

where \mathbf{p} is a vector of mode parameters: ν_0 , A , w , b and N_a a-coefficients.

may optionally include a parameter to describe mode profile asymmetry, but we shan't get into that :)

Inversions

use a regularized least squares (RLS) inversion; minimize errors while penalizing wildly oscillating solutions:

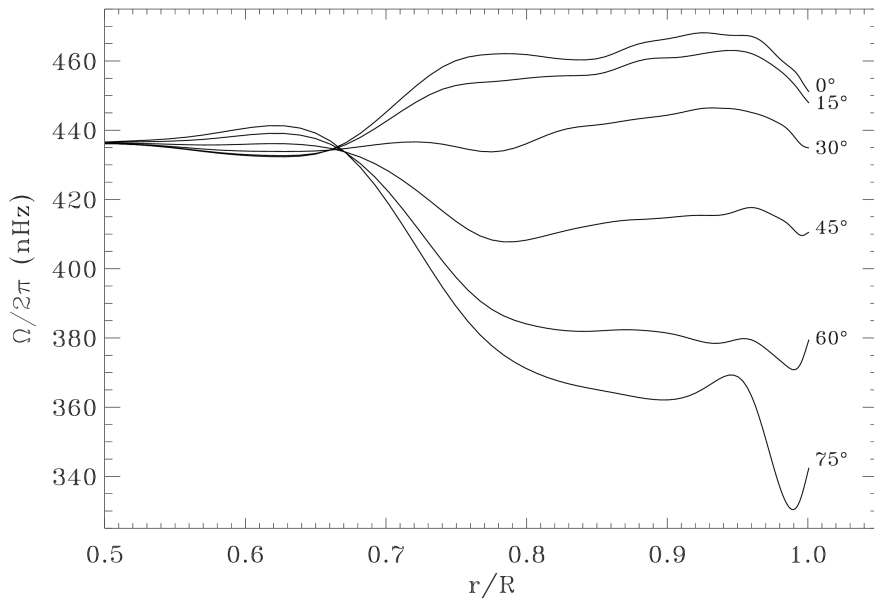
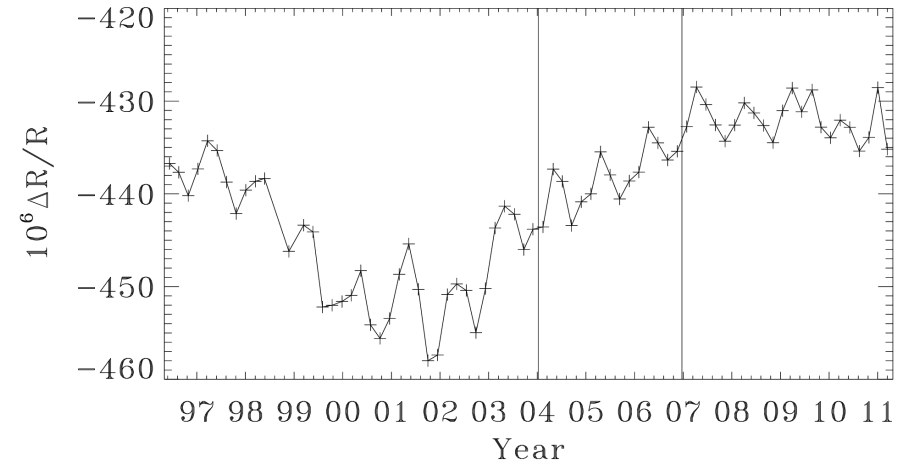
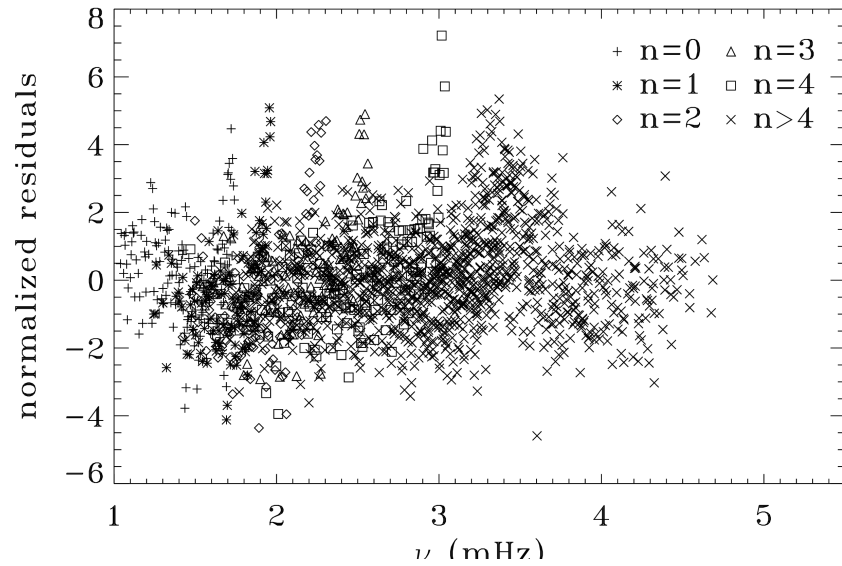
$$\sum_{n\ell} \left[\frac{1}{\sigma_1(n, \ell)} \left(\int_0^1 K_{n\ell}(r) \bar{\Omega}(r) dr - a_1(n, \ell) \right) \right]^2 + \mu \int_0^1 \left(\frac{d^2 \bar{\Omega}}{dr^2} \right)^2 dr$$

where $\bar{\Omega}$ is the inferred rotation rate, K are known kernels, and μ is the tradeoff parameter controlling the importance of the two terms.

or in two dimensions:

$$\sum_{n\ell s} \left[\frac{1}{\sigma_{2s+1}(n, \ell)} \left(\int_0^1 \int_0^\pi K_{n\ell s}(r, \theta) \bar{\Omega}(r, \theta) dr d\theta - a_{2s+1}(n, \ell) \right) \right]^2 + \mu_r \int_0^1 \left(\frac{d^2 \bar{\Omega}}{dr^2} \right)^2 dr + \mu_\theta \int_0^\pi \left(\frac{d^2 \bar{\Omega}}{d\theta^2} \right)^2 d\theta$$

Problems with the MDI vw_V Data



Bump
Jet

Horns
Annual Period

tried 10 different improvements

corrected for: image scale, cubic distortion, CCD misalignment, inclination error, CCD tilt

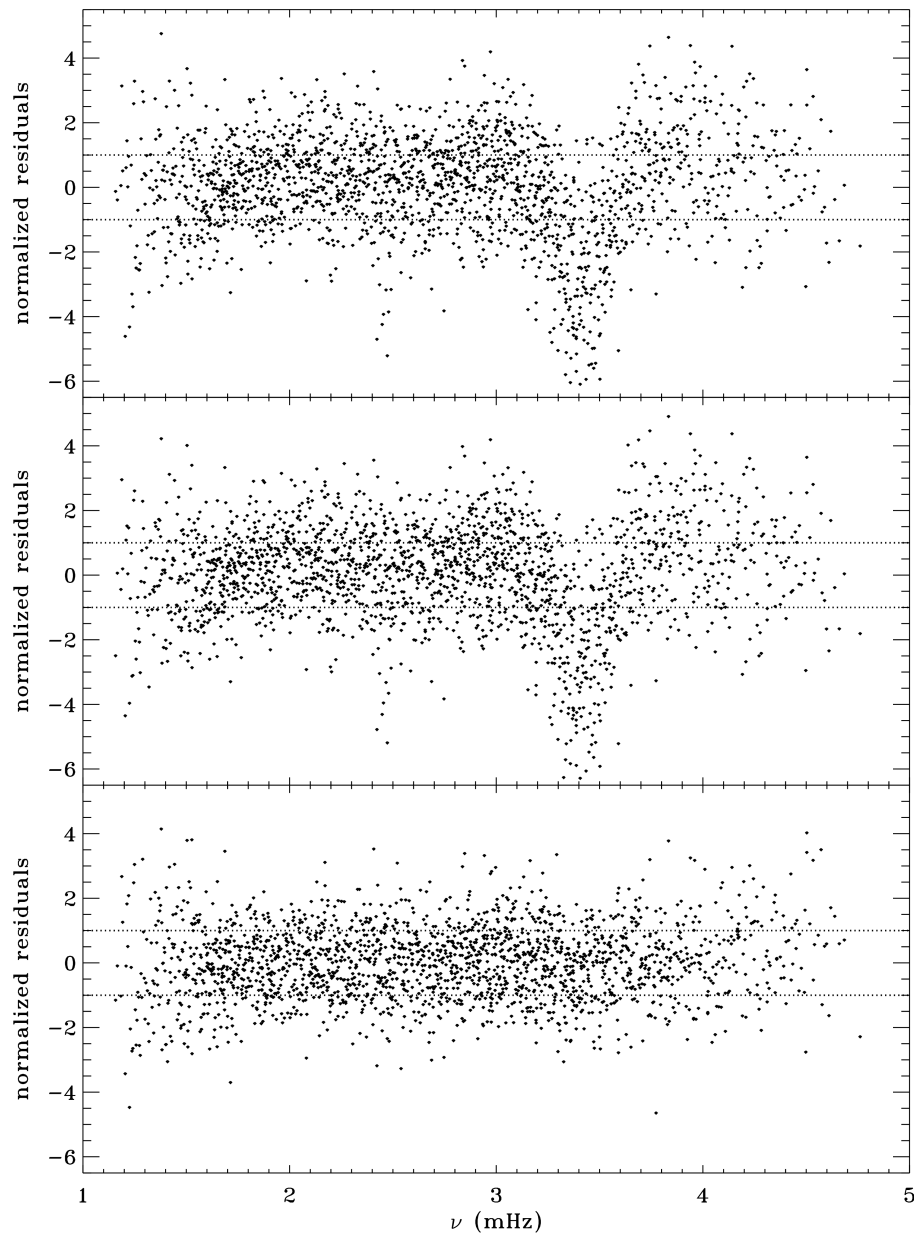
updated: window functions, detrending, gapfilling

Accounted for: horizontal displacement, distortion of eigenfunctions, mode profile asymmetry

Progress: eliminated horns,
 reduced annual period

No progress: bump,
 jet,
 six month period

Comparison with Full-Disk



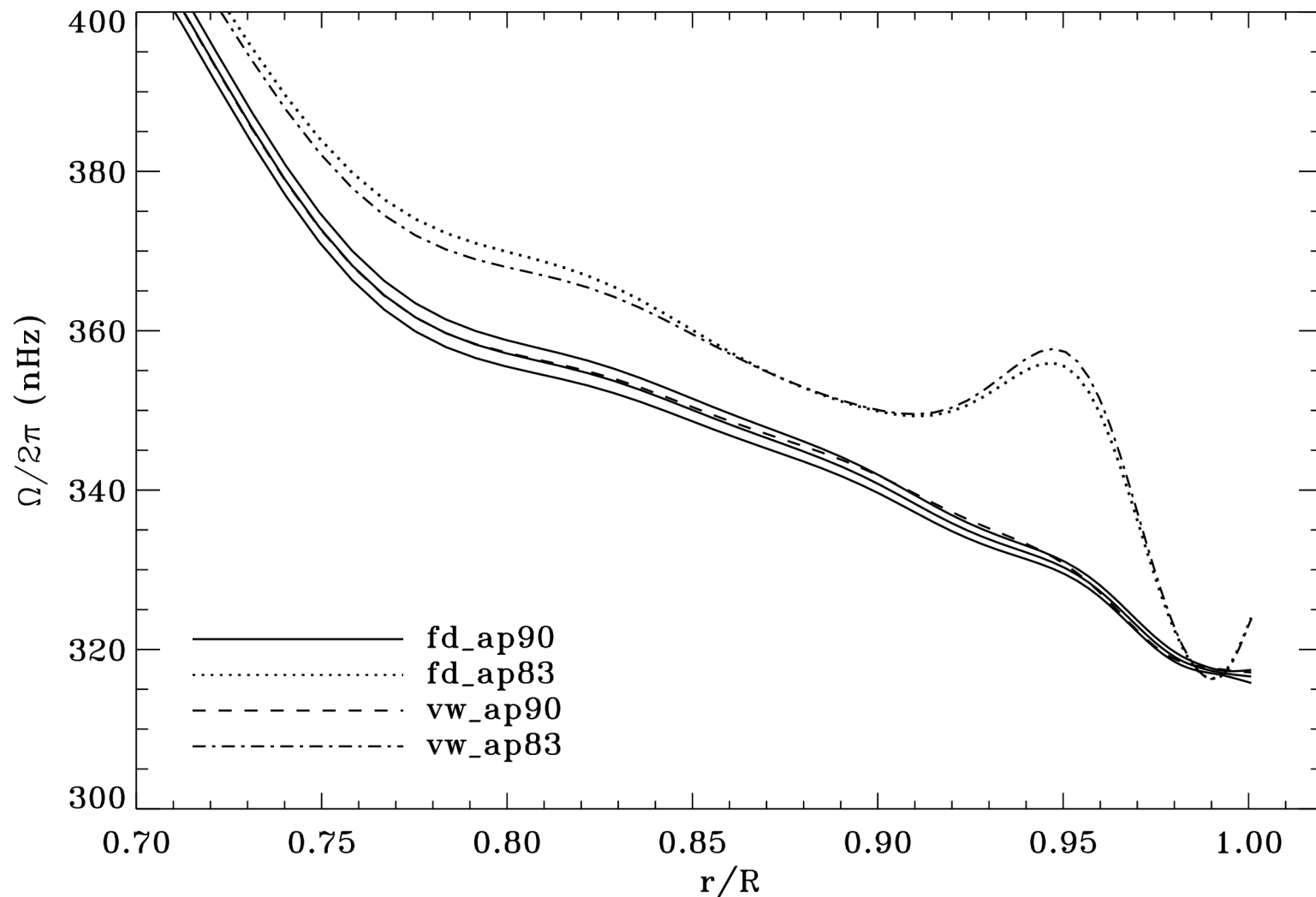
νw_V

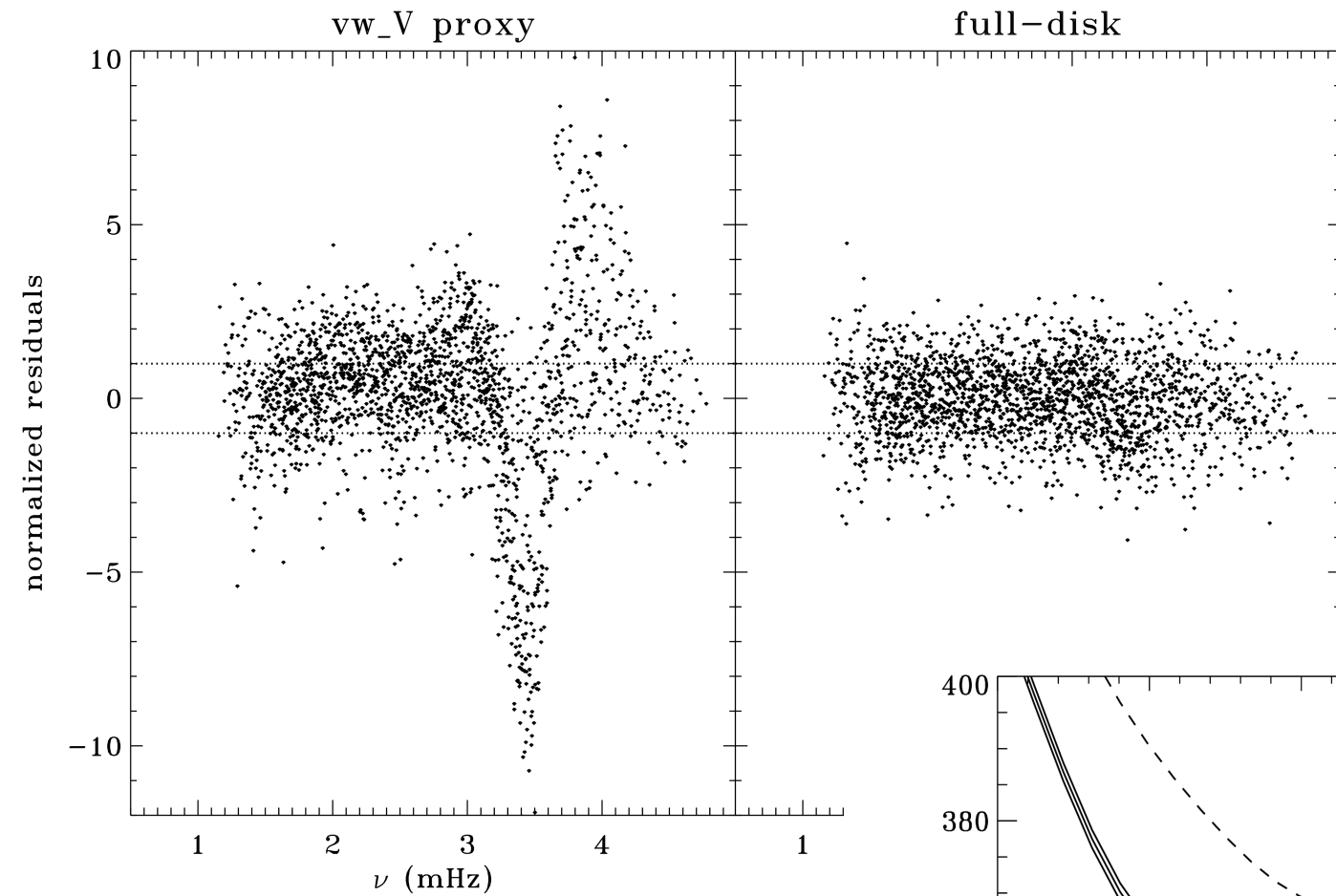
full-disk with νw_V
apodization

regular full-disk

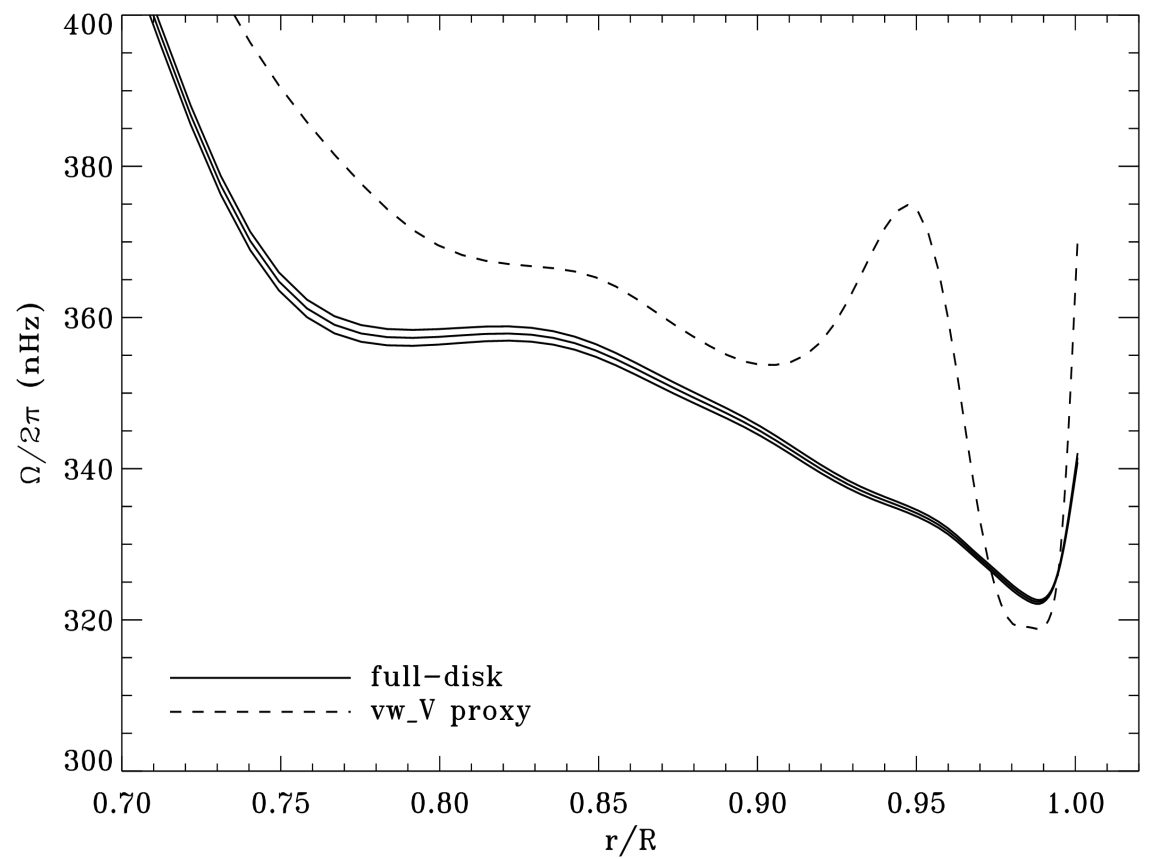
Above plots are for an average over dynamics runs. For 1998, we could use full-disk apodization on reconstructed vw_V . Resulting rotation rate at 75° latitude:

Solid lines show regular full-disk analysis and its errors; errors for the other analyses were similar.

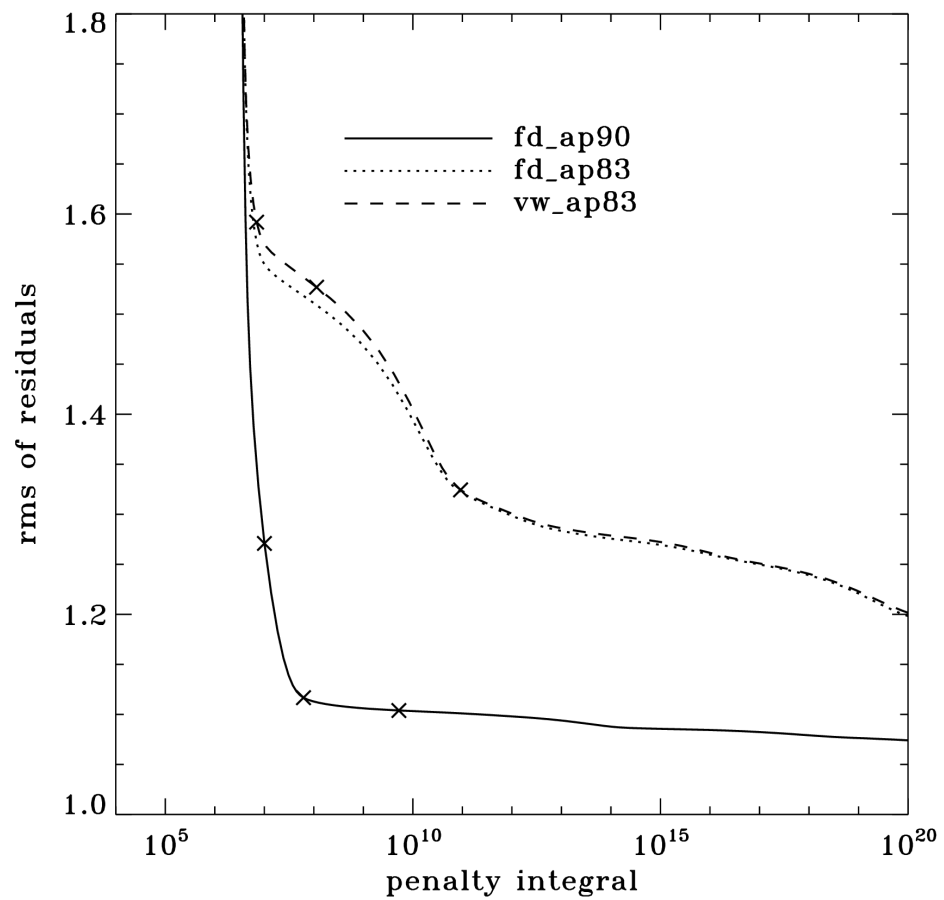




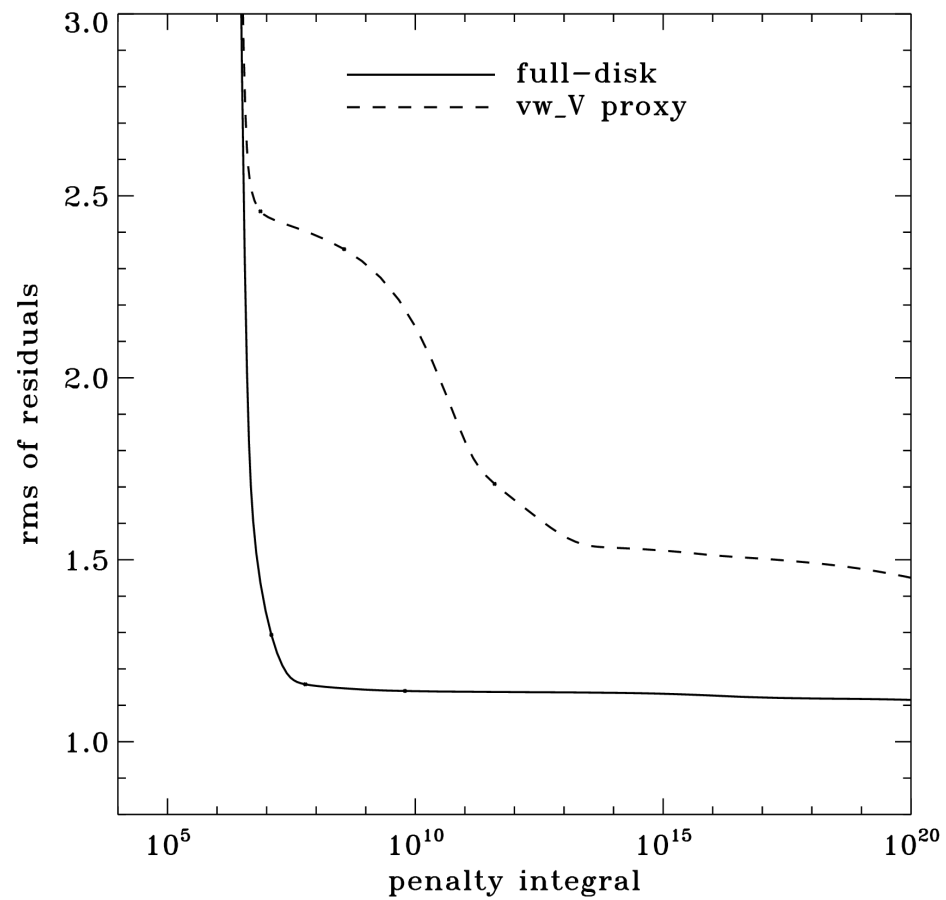
Average HMI



Tradeoff Curves



MDI

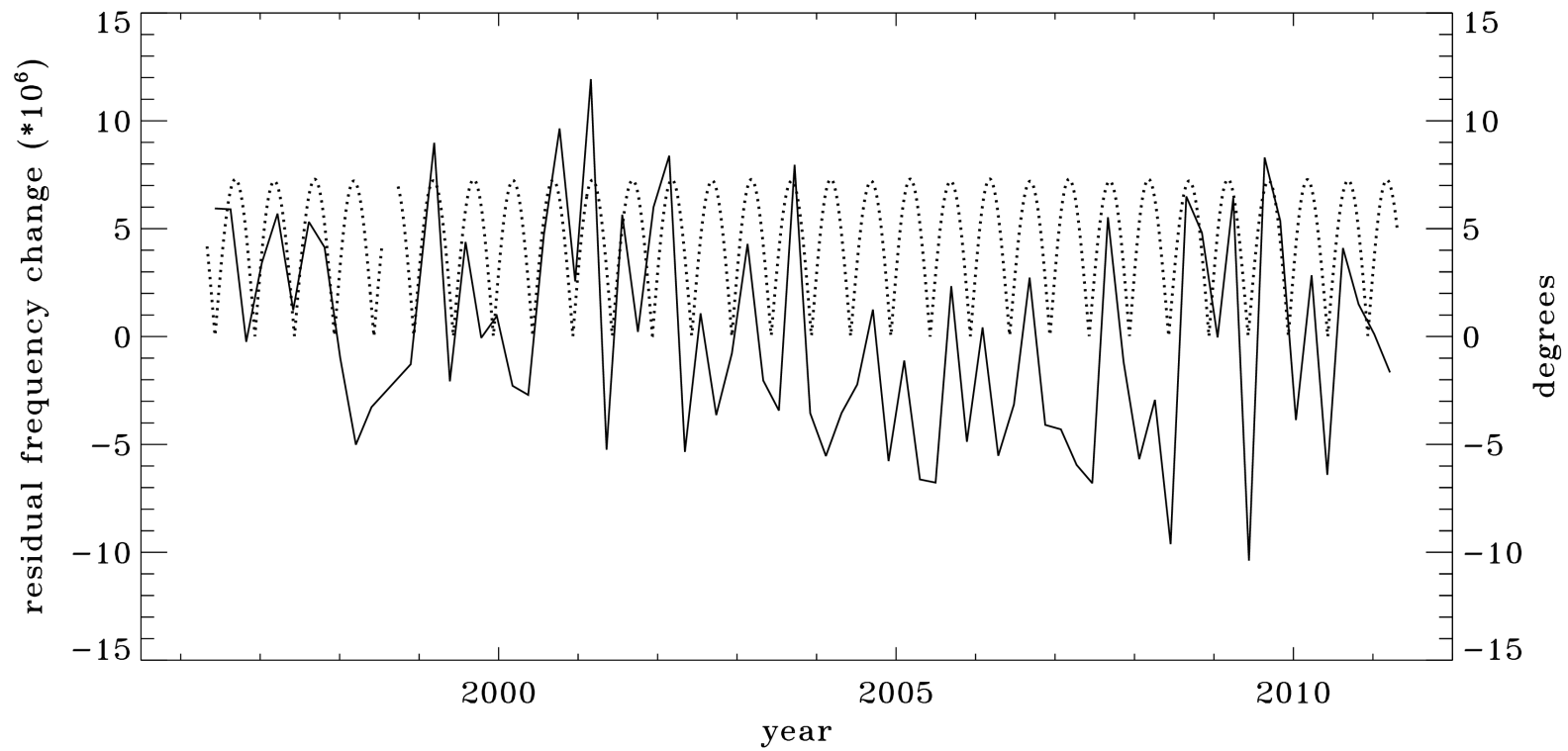
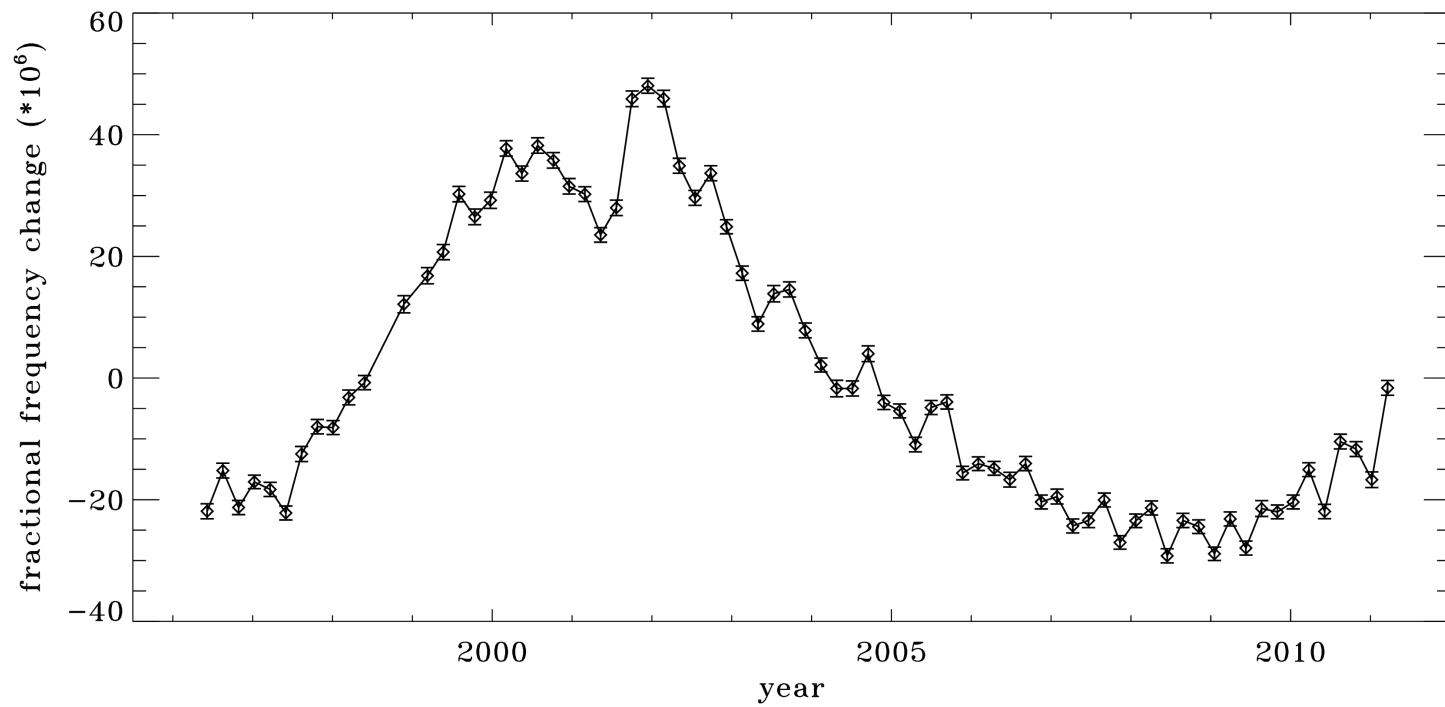


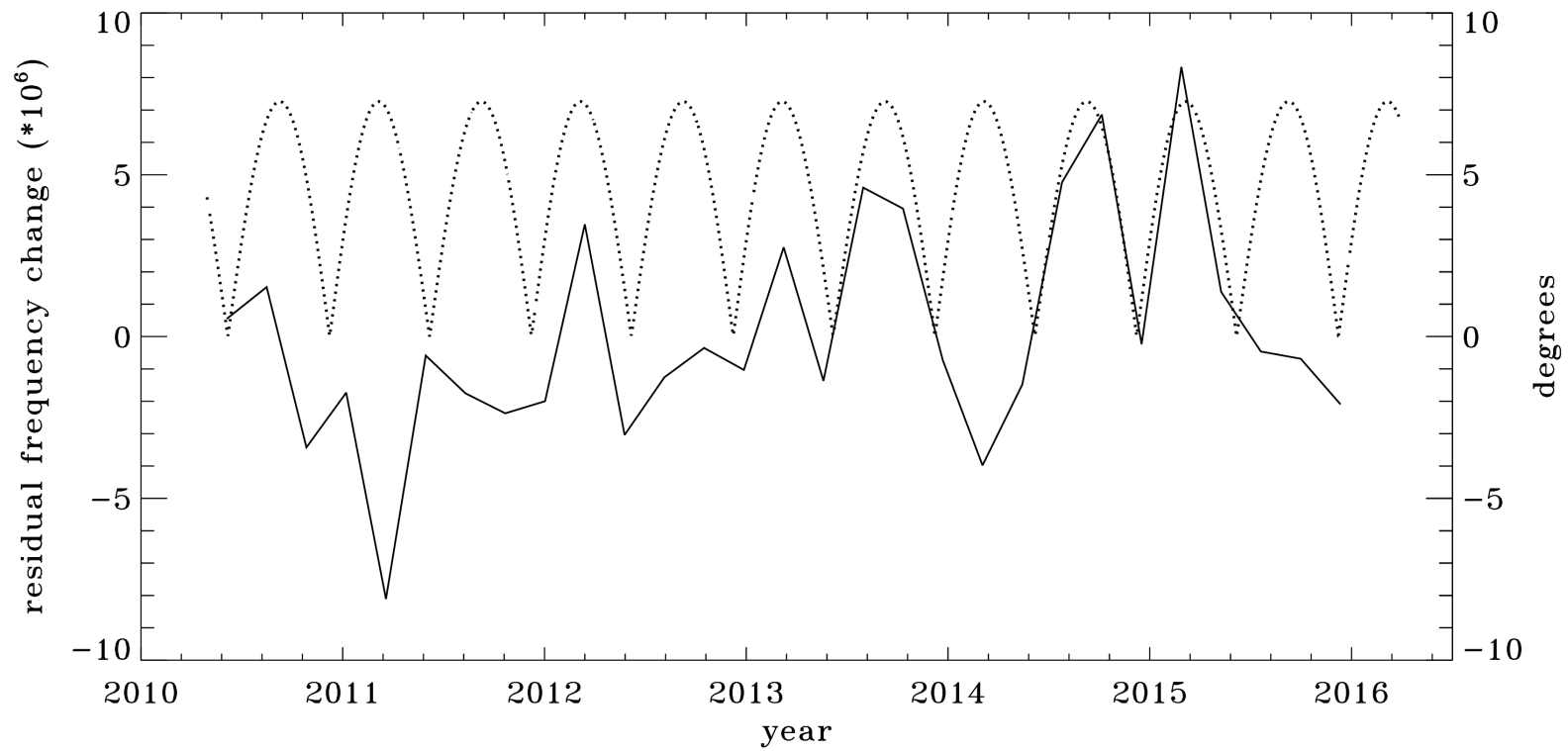
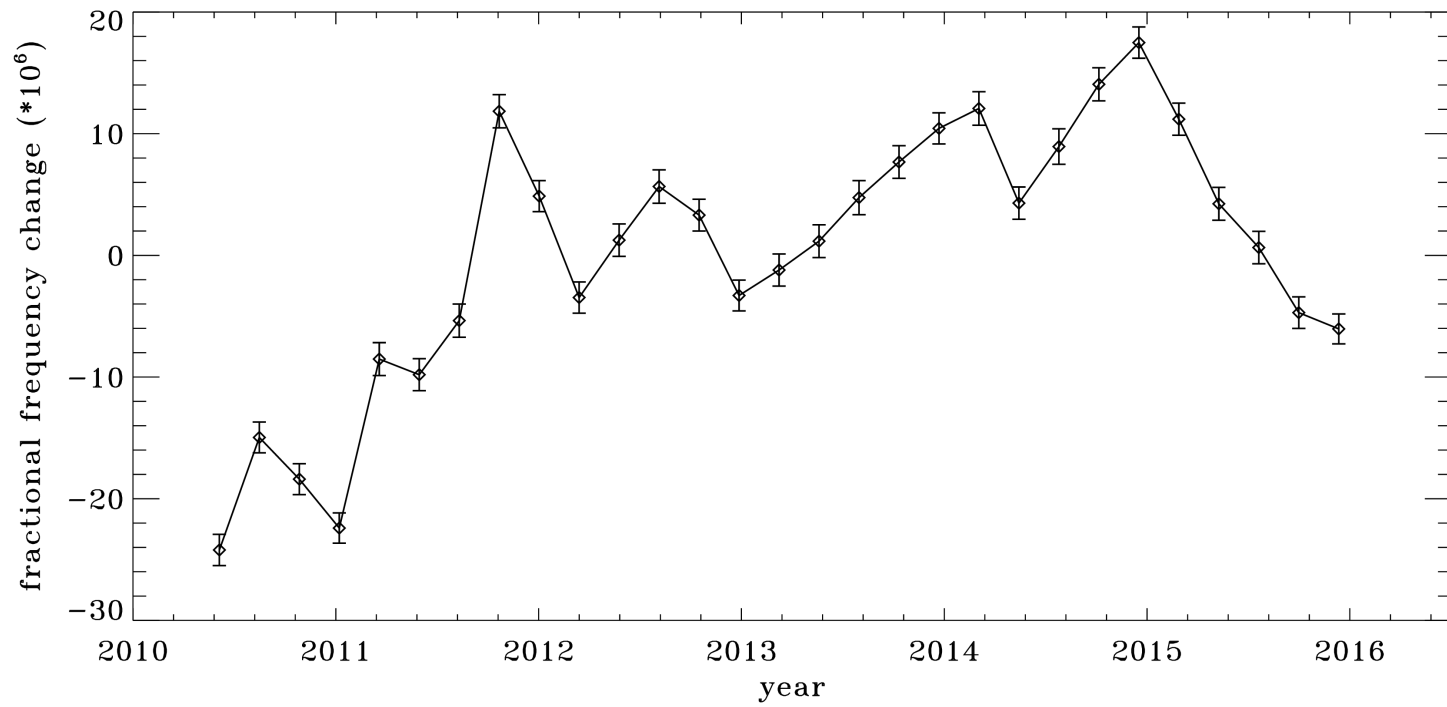
HMI

Periodicity

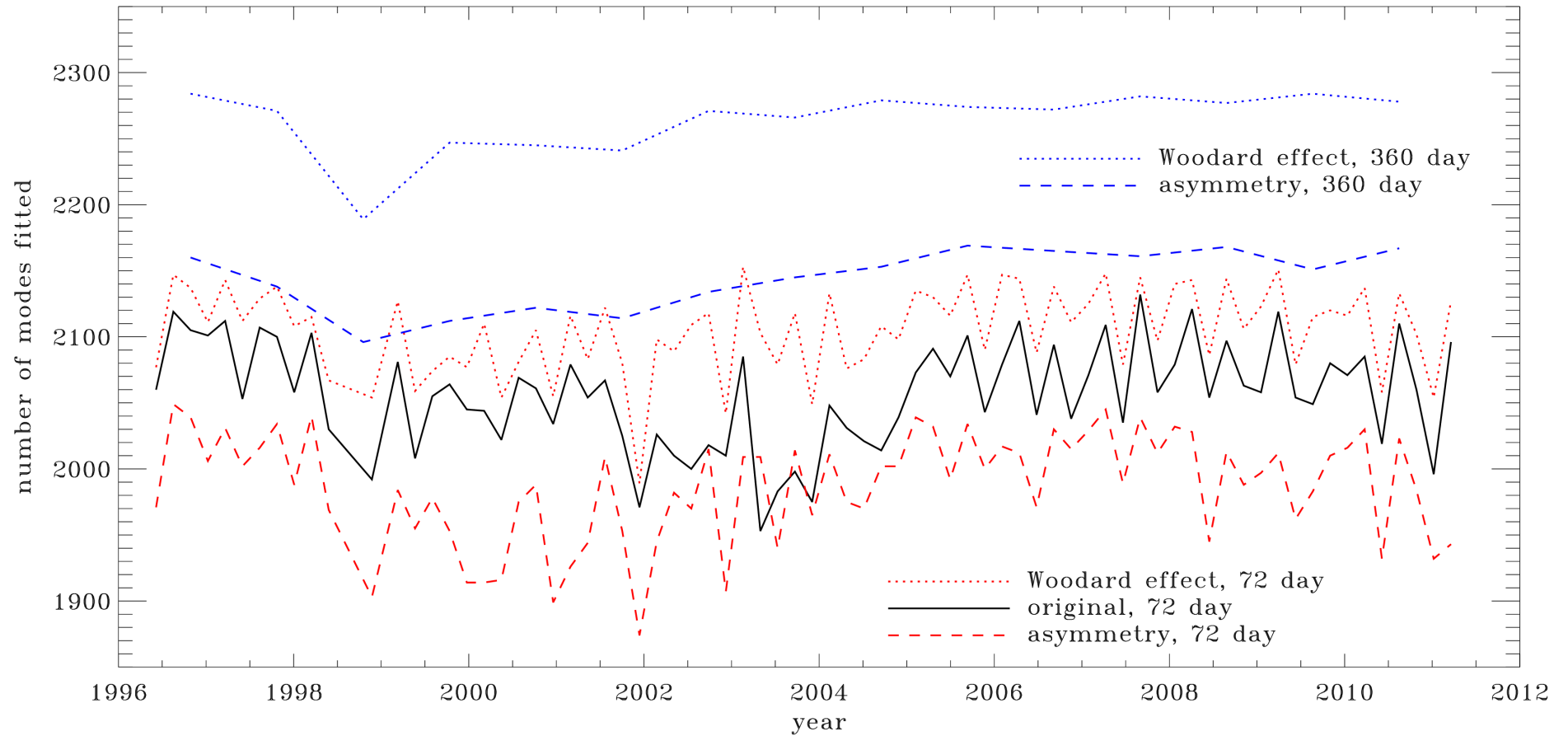
Fractional change in seismic radius is proportional to fractional change in f-mode frequencies, in which MDI sees a prominent one-year period.

To investigate, we fit a line to the frequency shifts as a function of the average rms of the corresponding magnetograms. After subtraction, we see a correlation with the absolute value of B_0 .

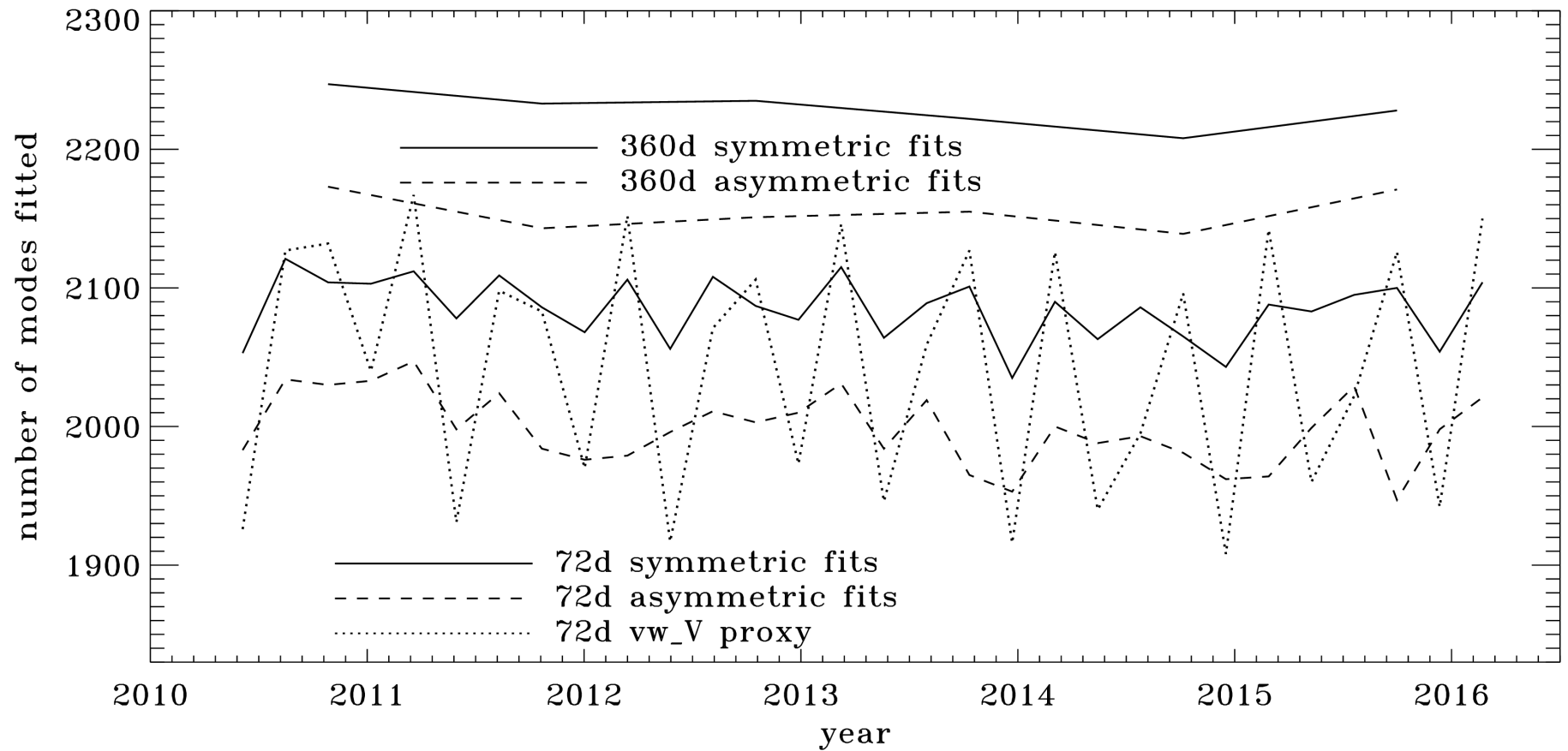




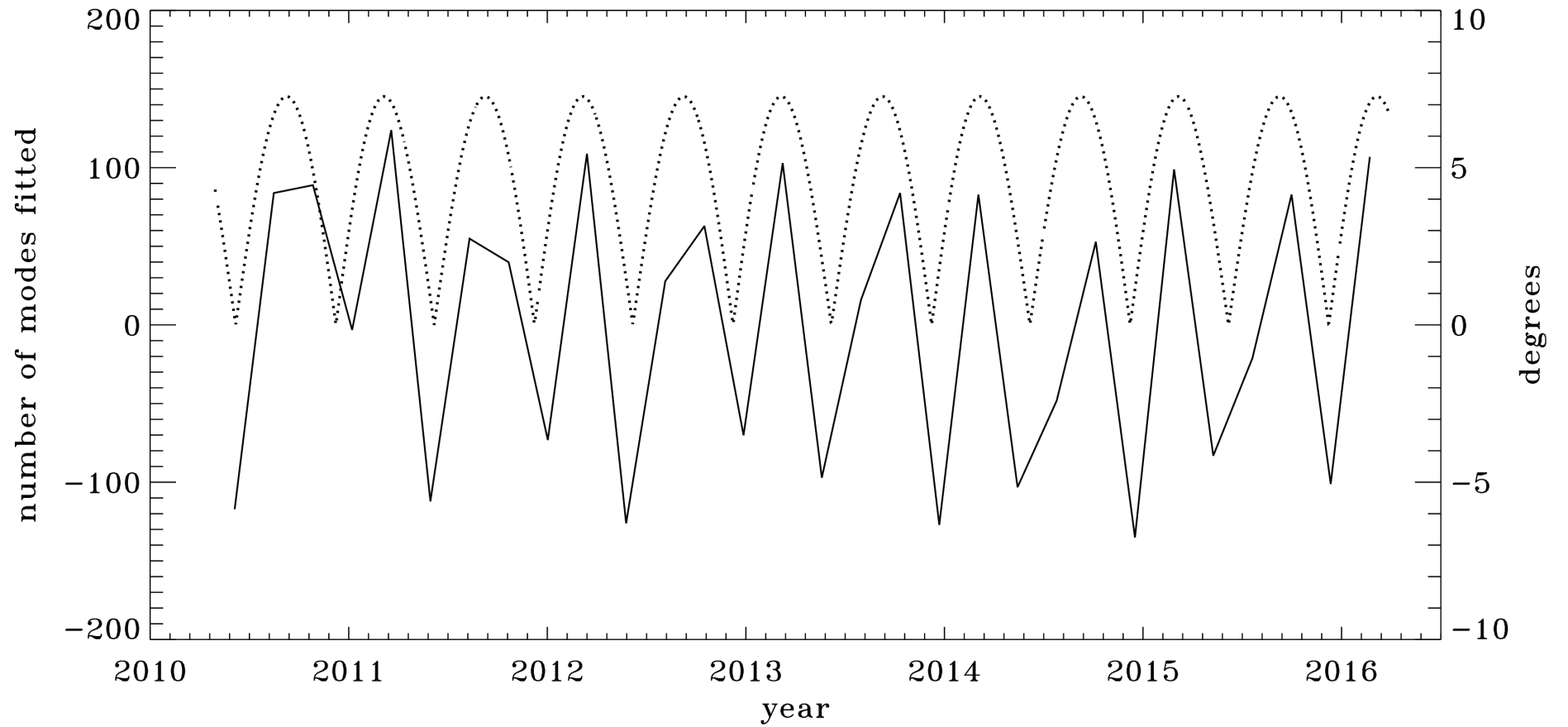
Mode Coverage: MDI



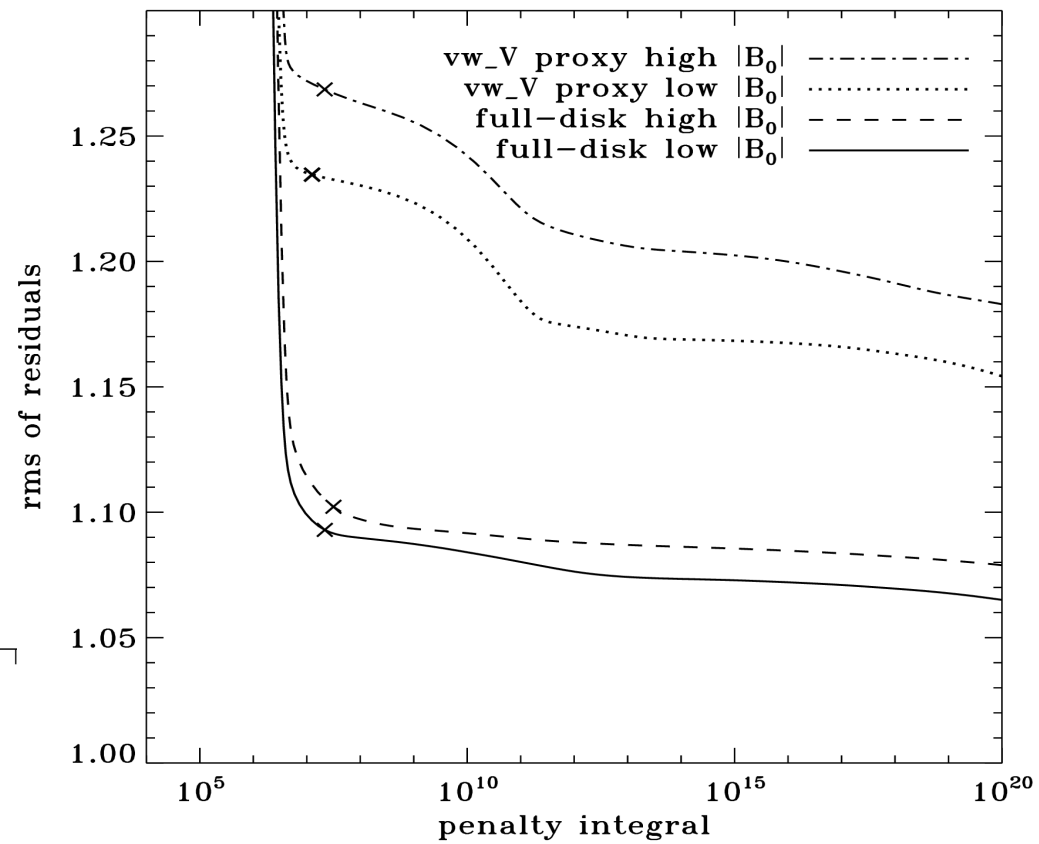
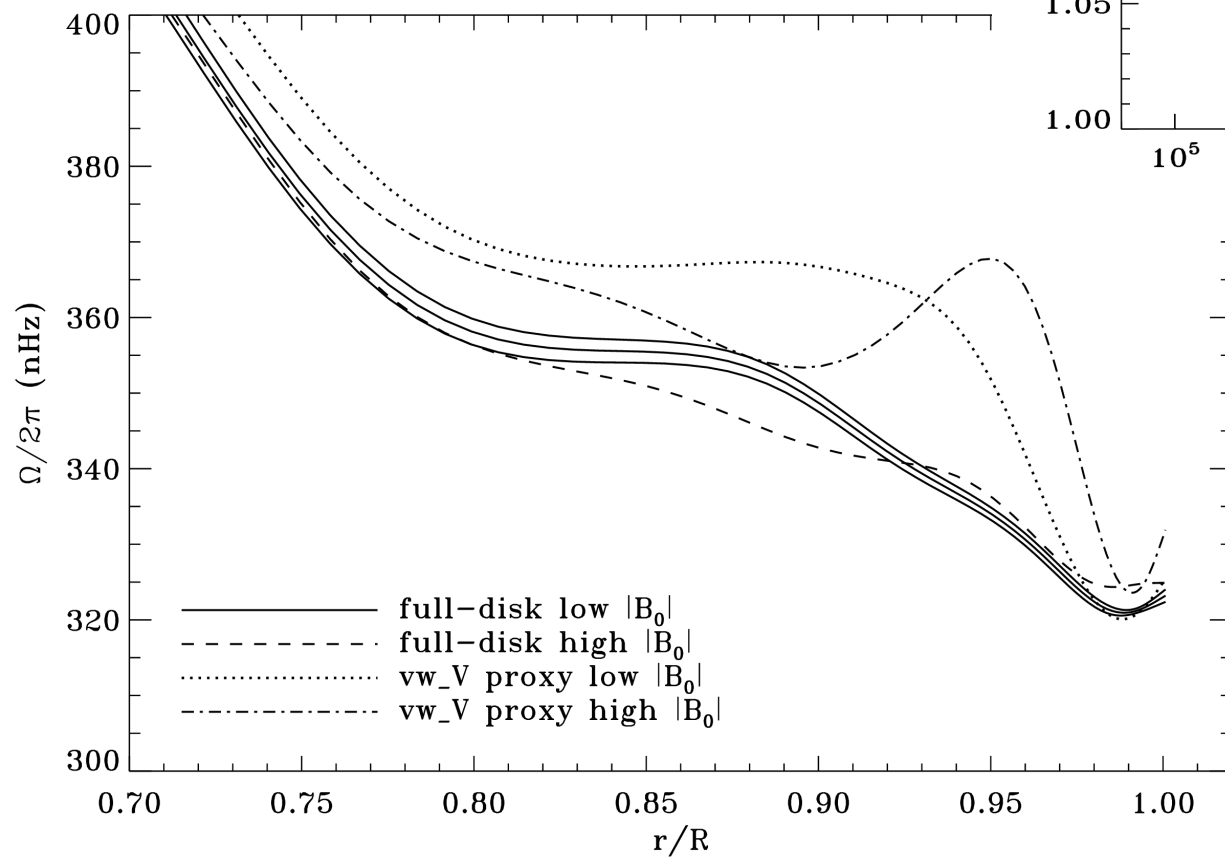
Mode Coverage: HMI



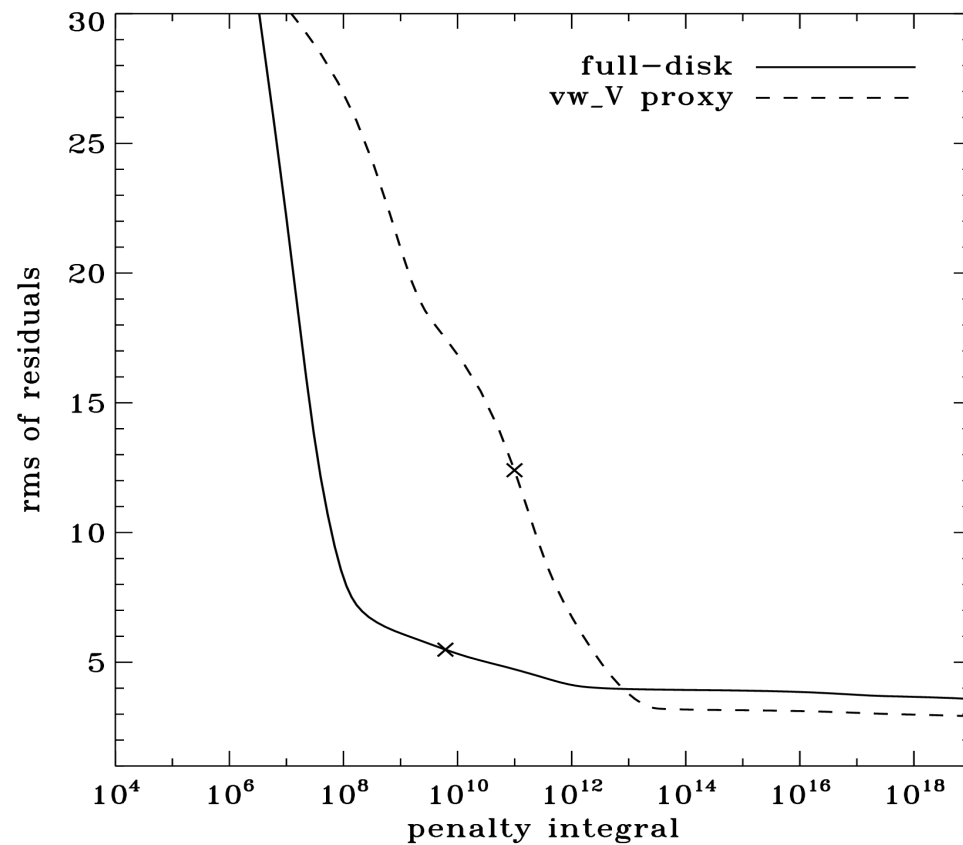
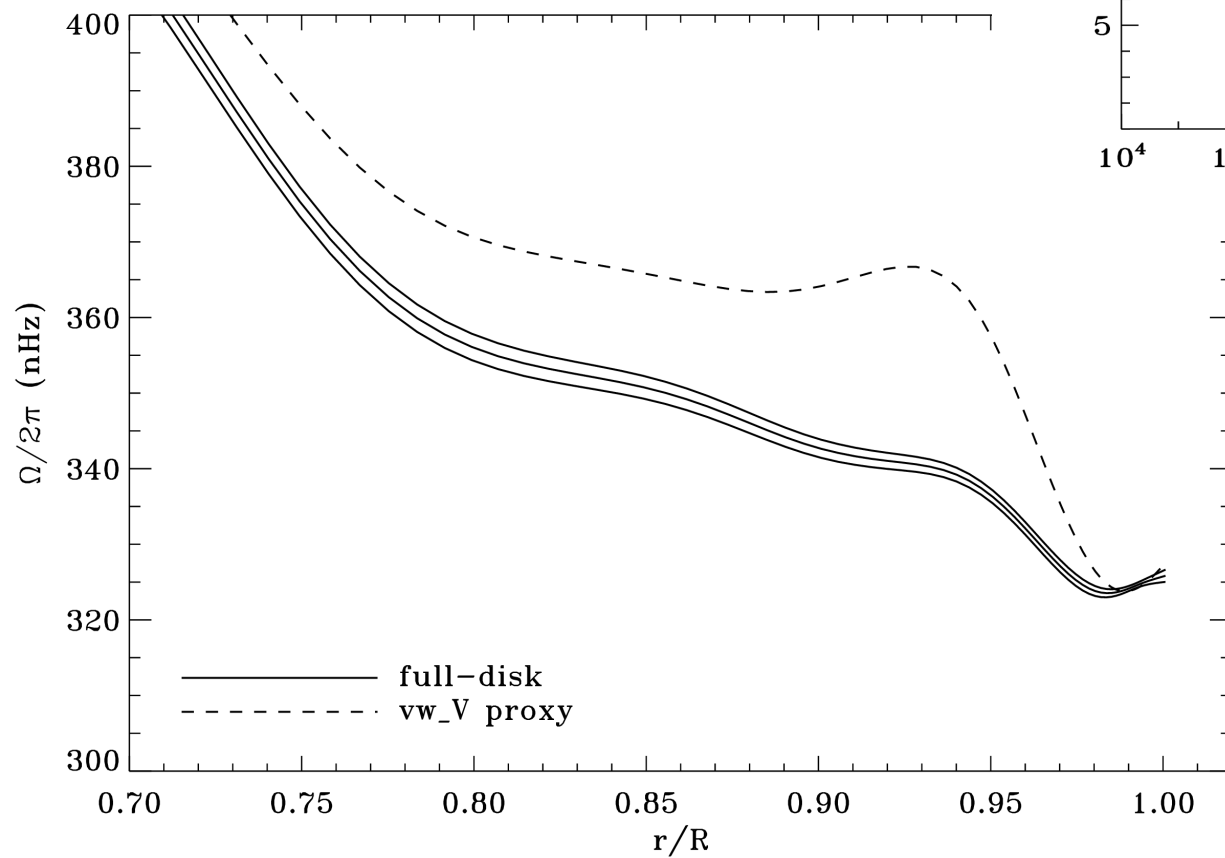
$|B_0|$ overplotted



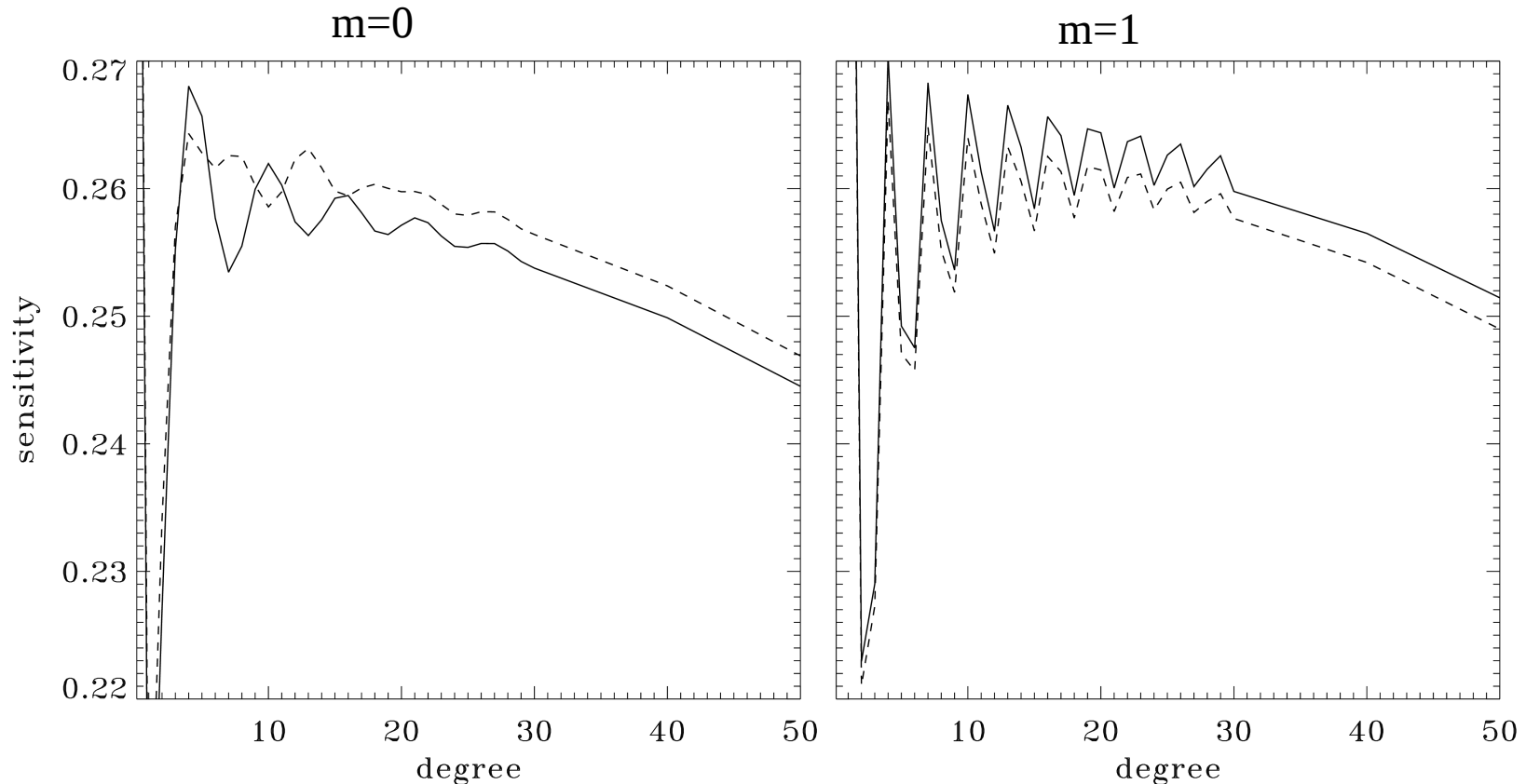
What?!?!



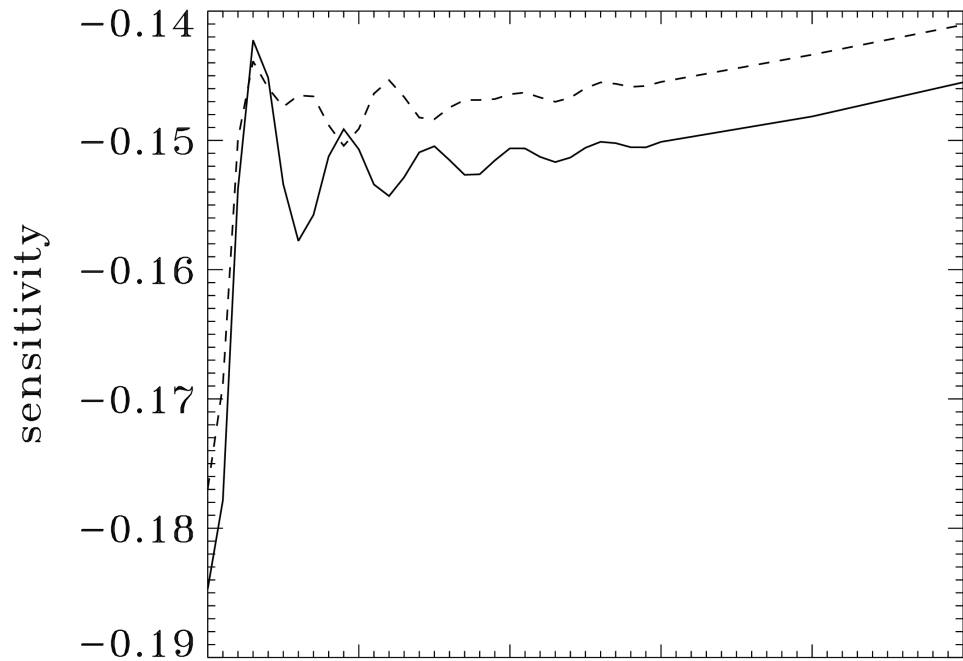
Common Modes



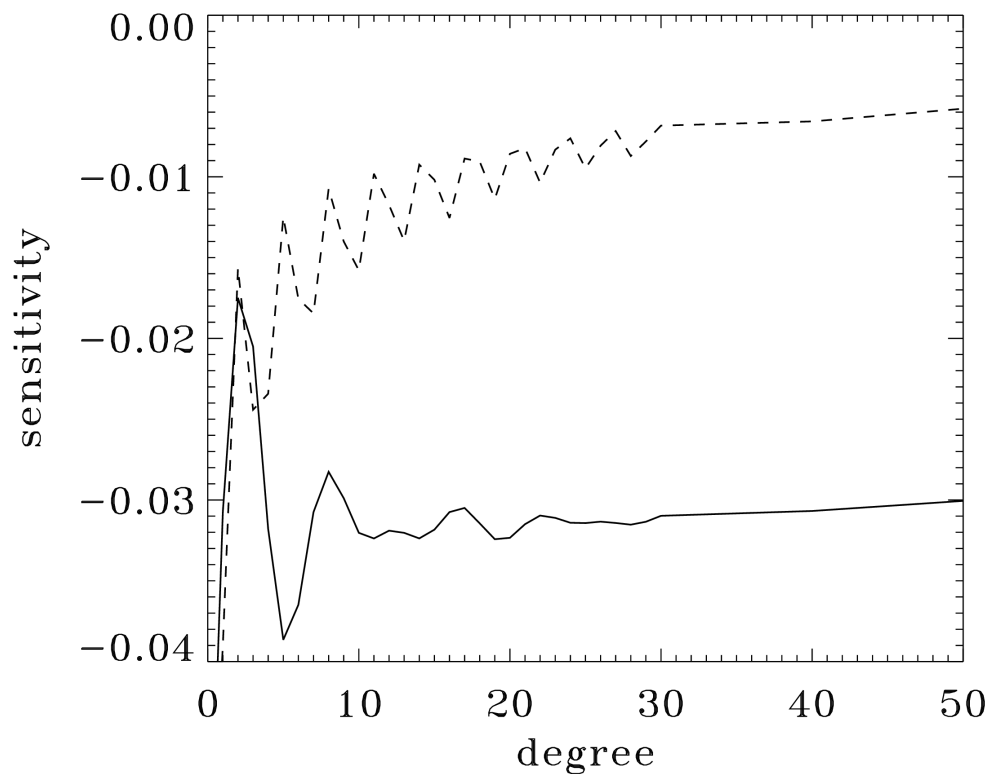
Leaks for nonzero B_0



Sensitivity to target mode. Solid lines show original leakage matrix, dashed lines show leaks calculated for high $|B_0|$.



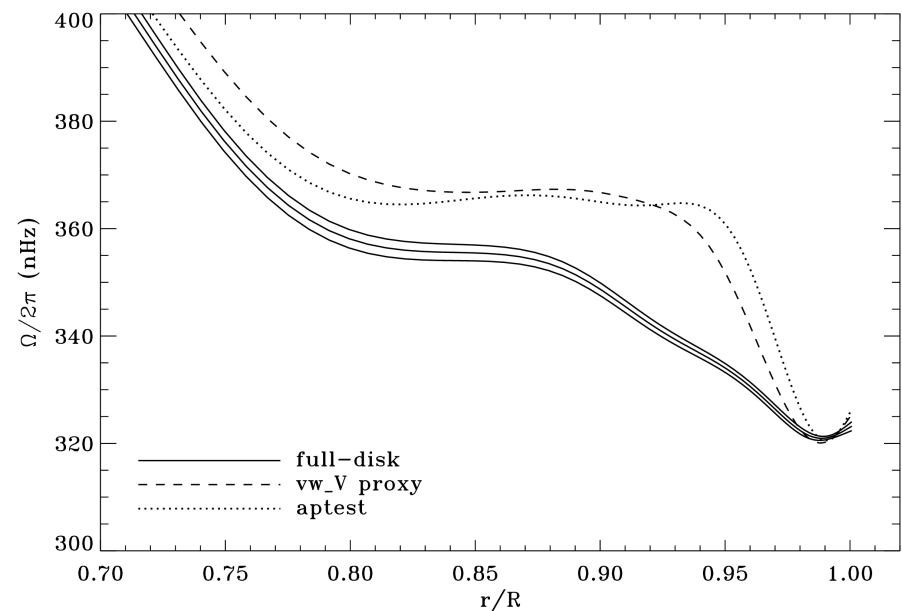
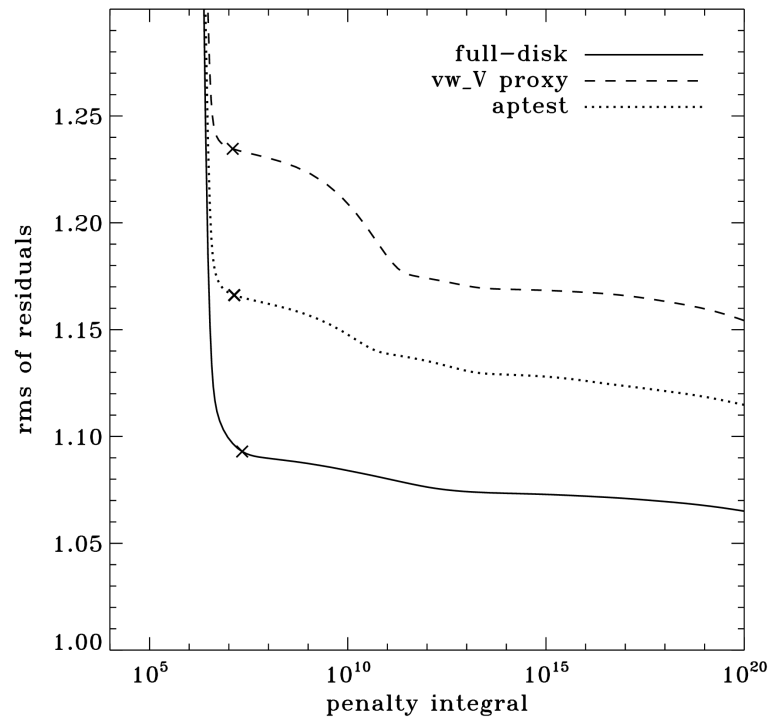
Leaks for $m=0$ and $\Delta l=2, \Delta m=0$. Solid line shows original, dashed line shows leaks for high $|B_0|$.

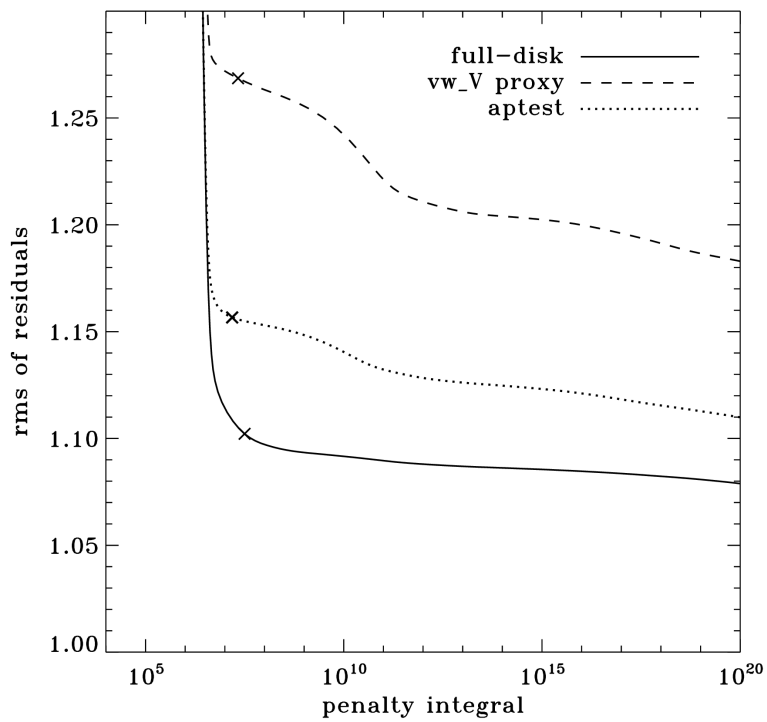


Leaks for high $|B_0|$, $\Delta l=1, \Delta m=0$. Solid line shows $m=0$, dashed line shows $m=1$. Original leaks are identically zero.

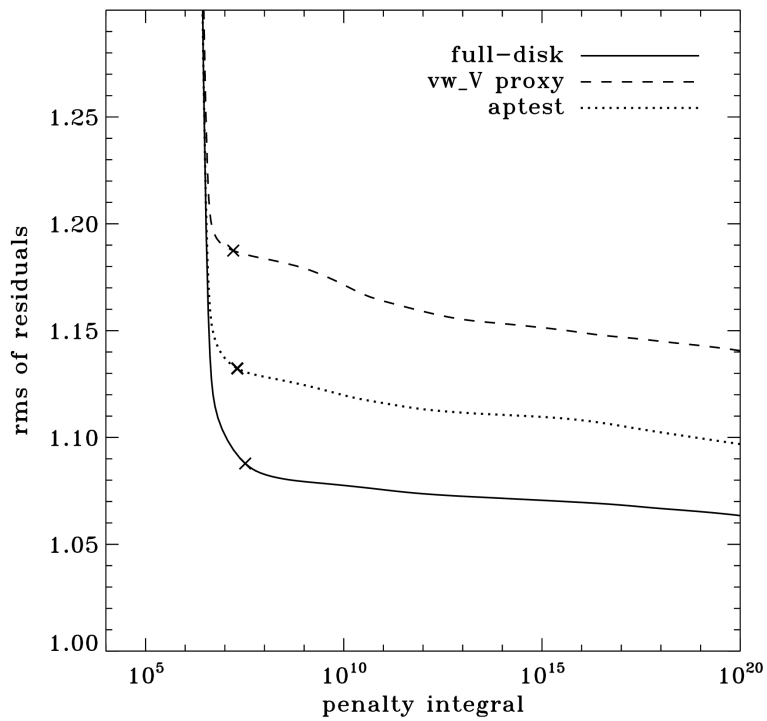
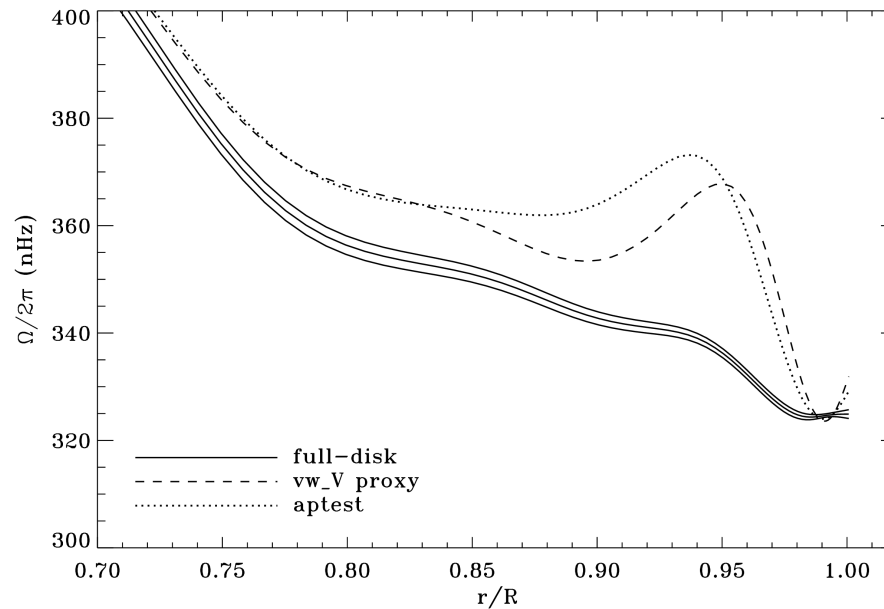
Our first test was to apodize in longitude from 54.1° to 60.5° with a hard cutoff in latitude at 60° . This would extend outside the crop radius at the corners, so an additional hard cutoff at an image radius of $0.88R$ was also imposed.

Low $|B_0|$

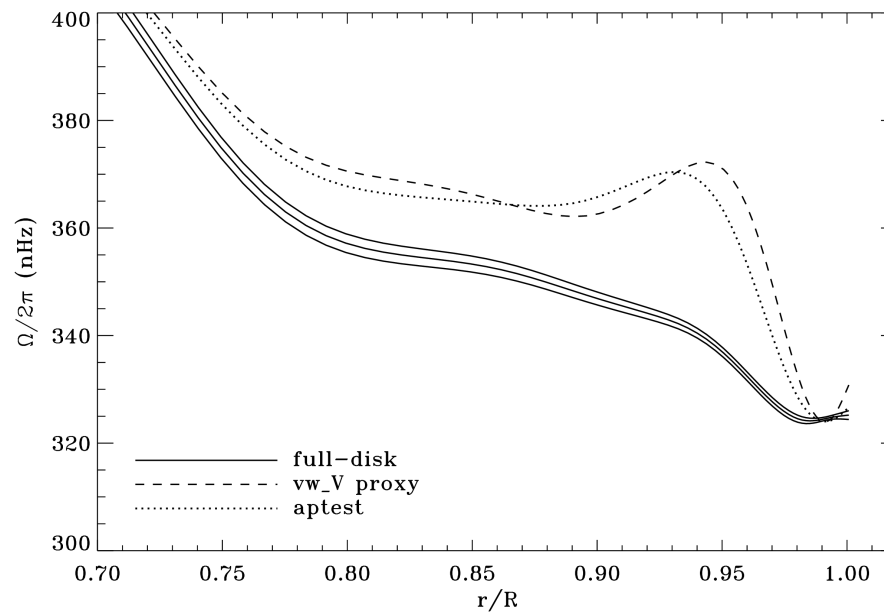




High $|B_0|$

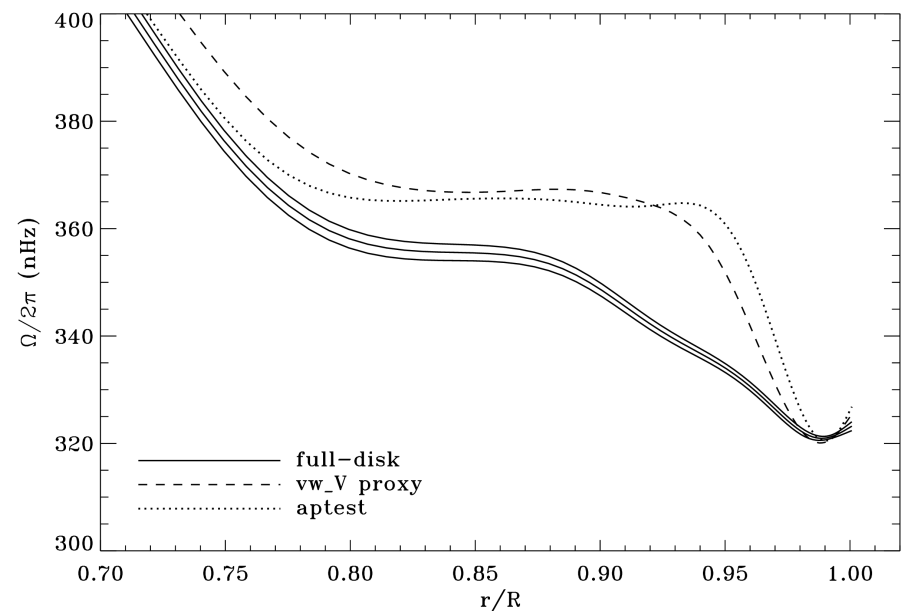
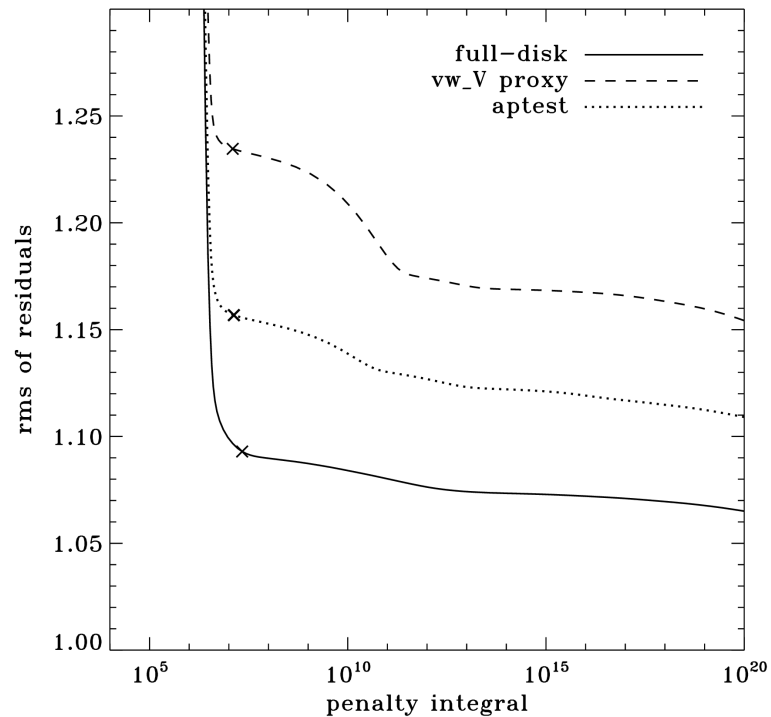


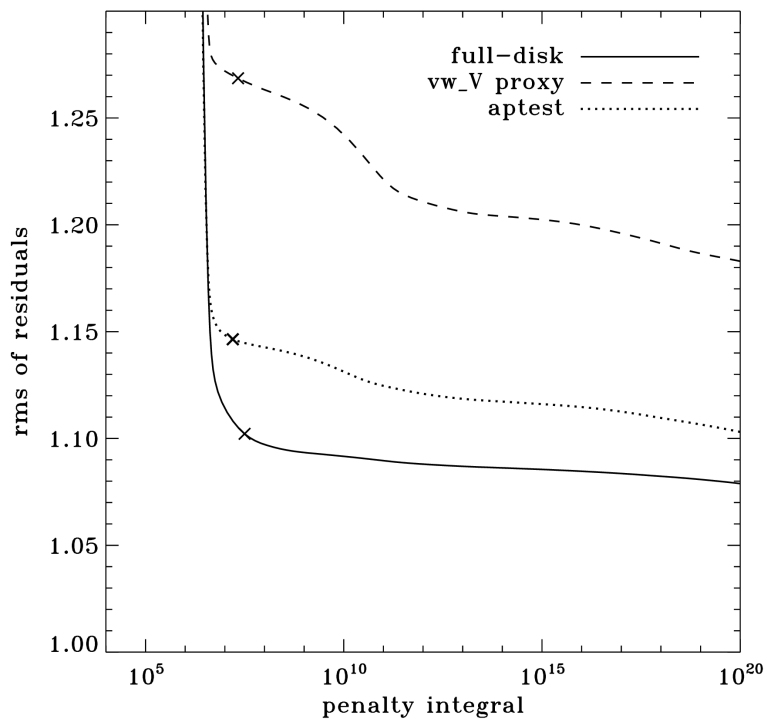
New Leaks



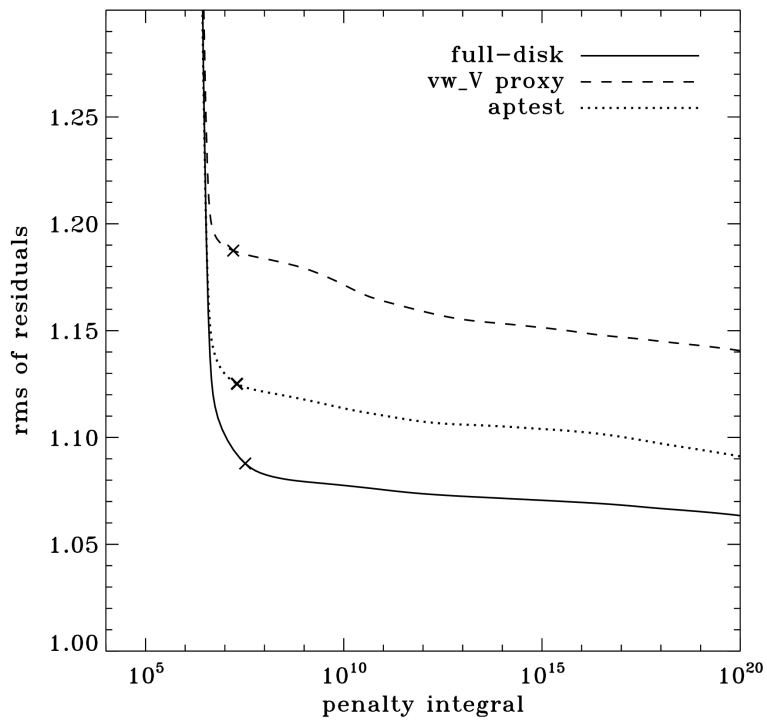
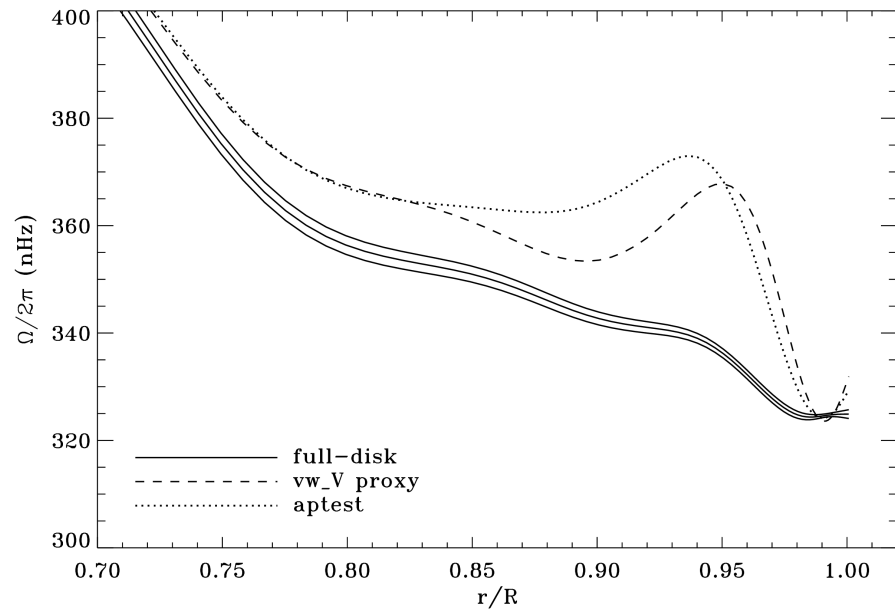
These results were mildly encouraging. Since the hard cutoff in latitude would be expected to spread power around, our next test apodized in latitude the same as in longitude, leaving the hard cutoff at $r=0.88R$.

Low $|B_0|$

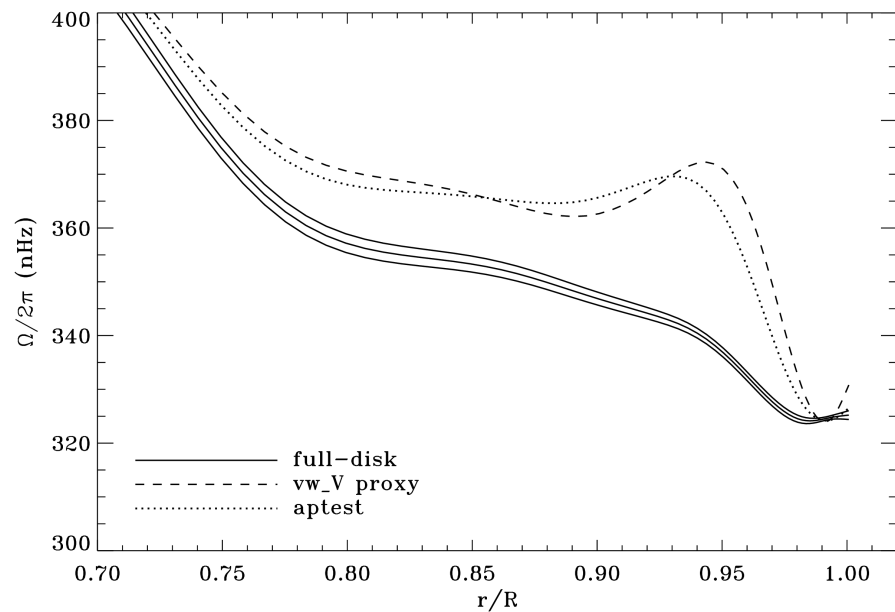




High $|B_0|$

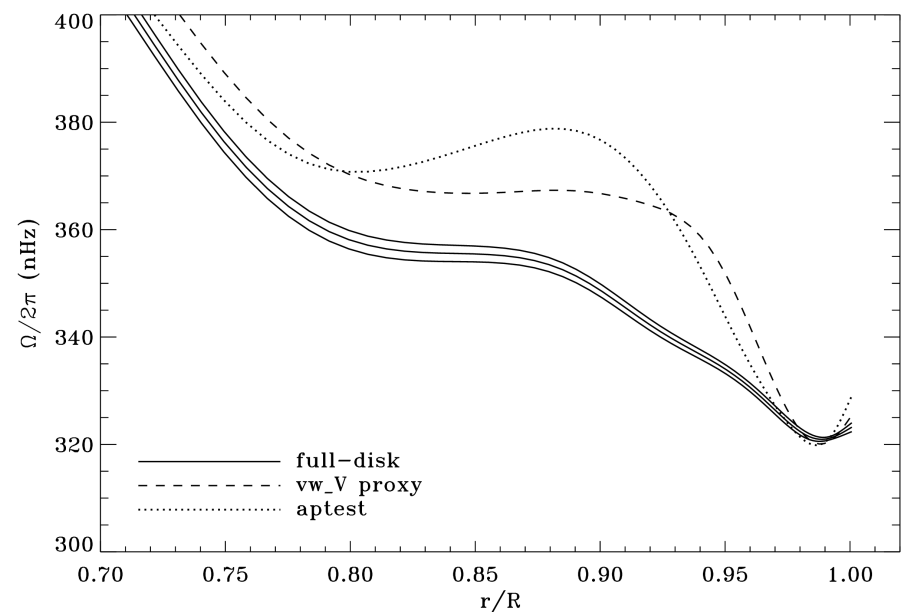
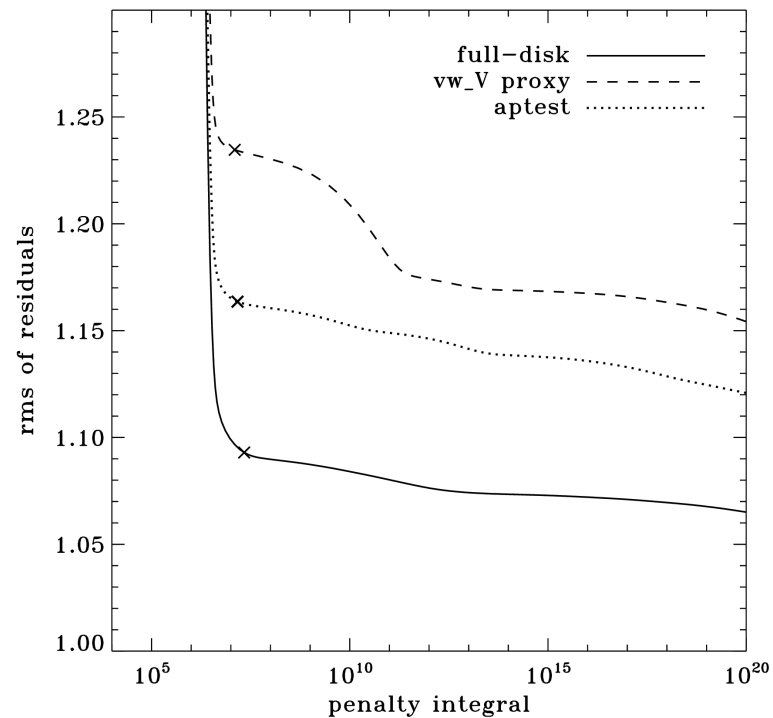


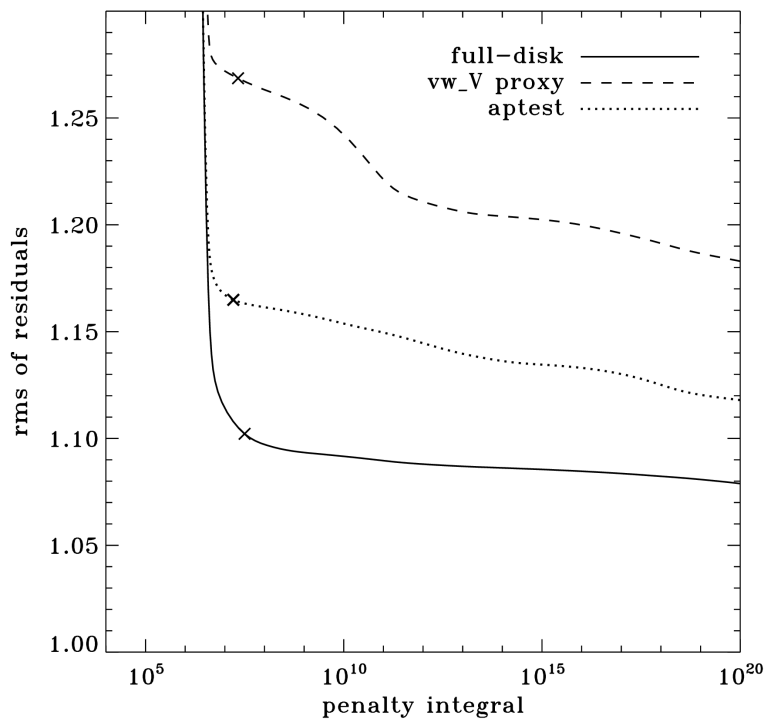
New Leaks



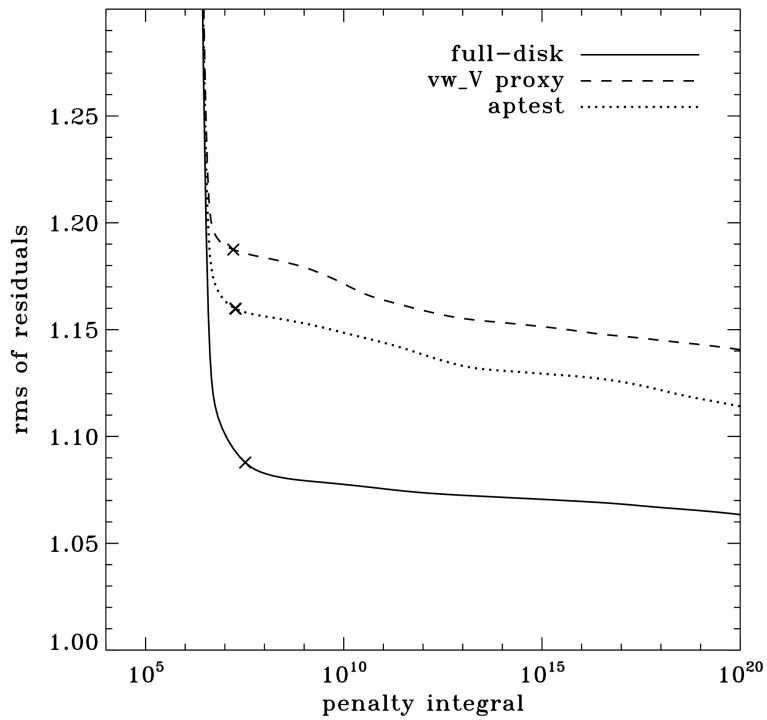
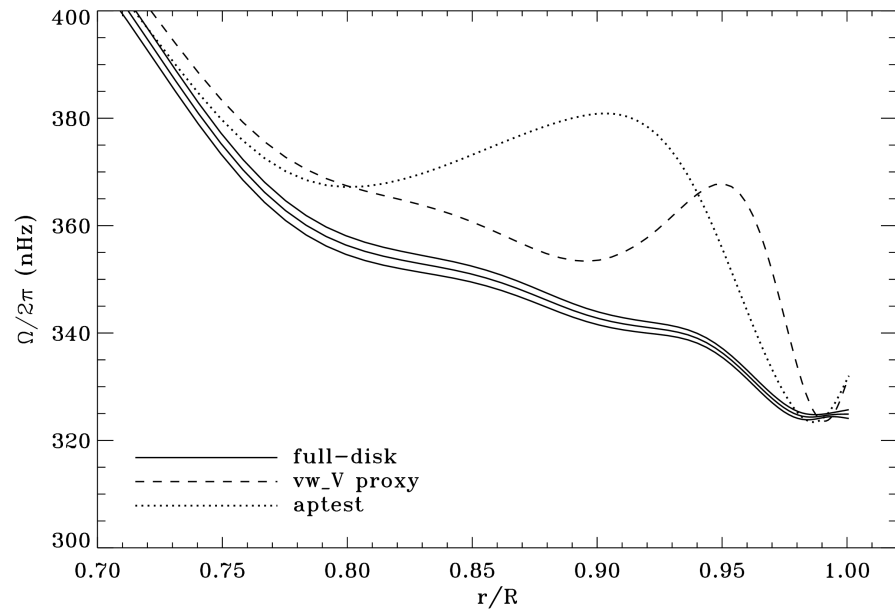
The residuals got even lower, but there was virtually no change in the rotation rates. For our next test we apodized more tightly in longitude and latitude, from 50.0° to 54.4° . This time we also apodize in fractional image radius from 0.87 to 0.88.

Low $|B_0|$

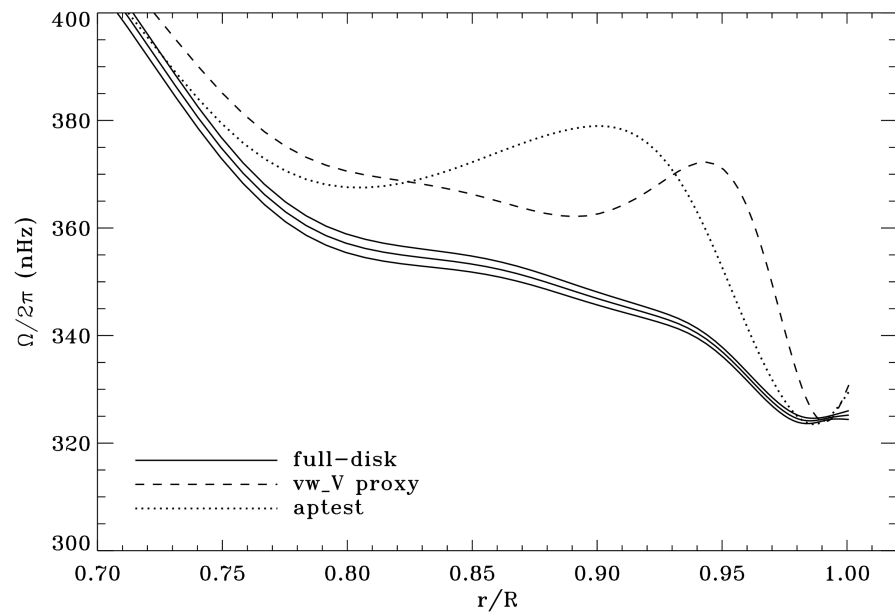




High $|B_0|$

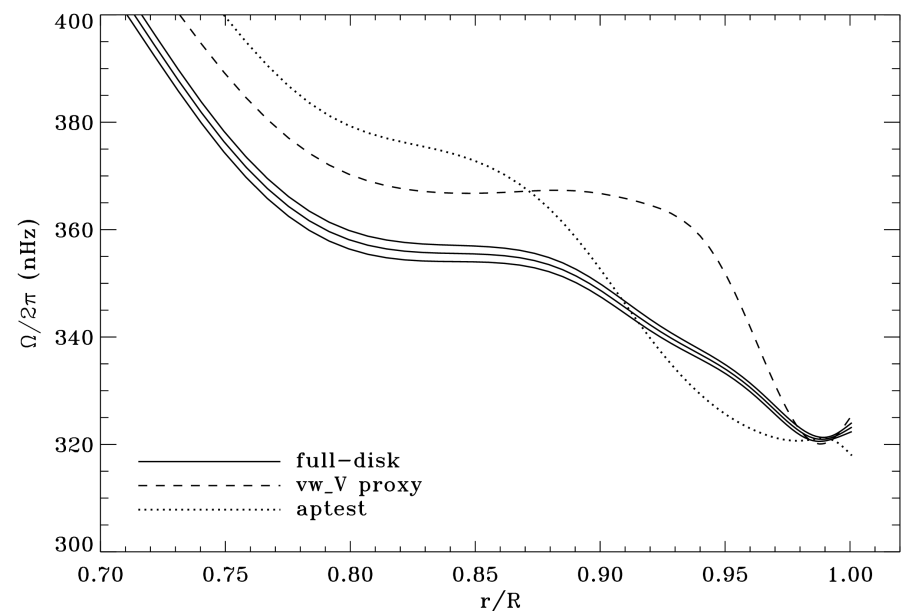
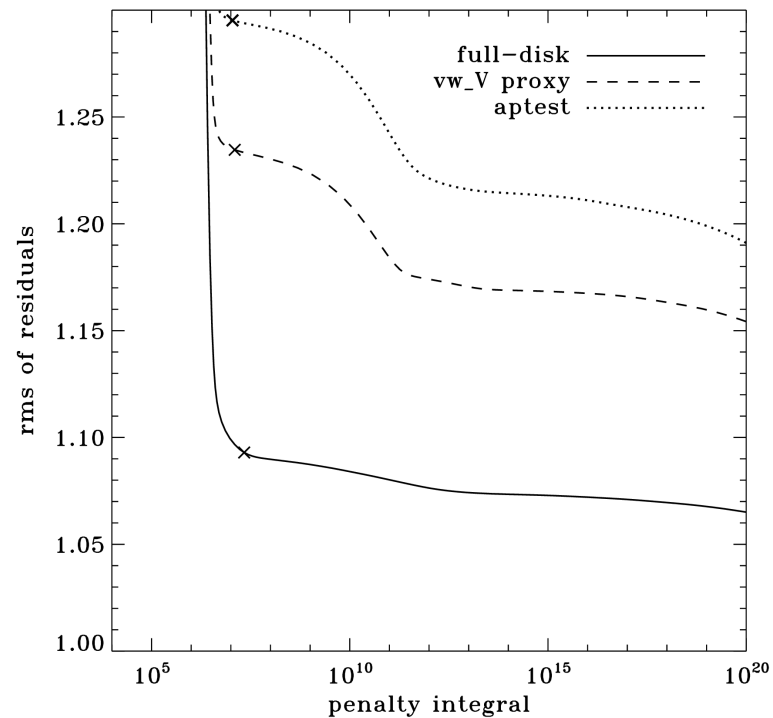


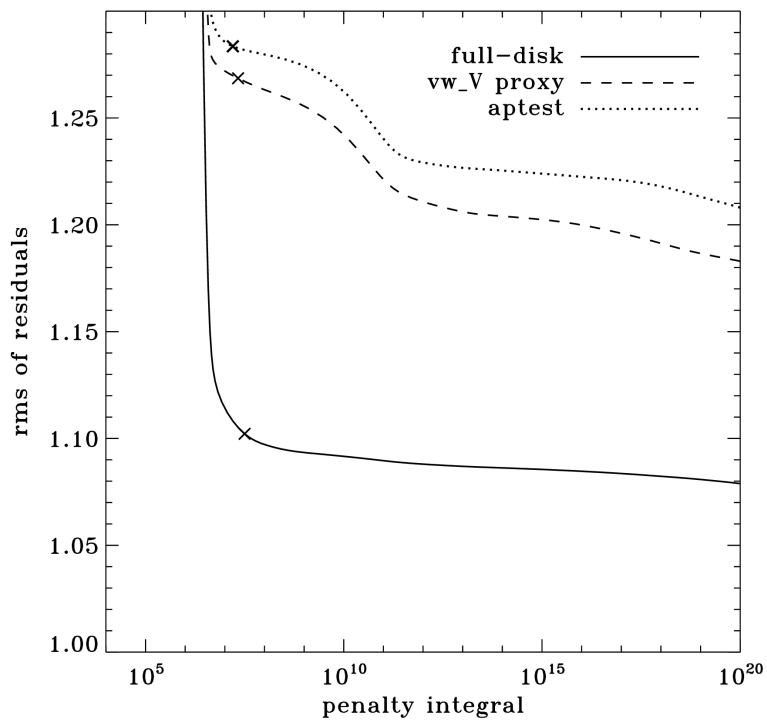
New Leaks



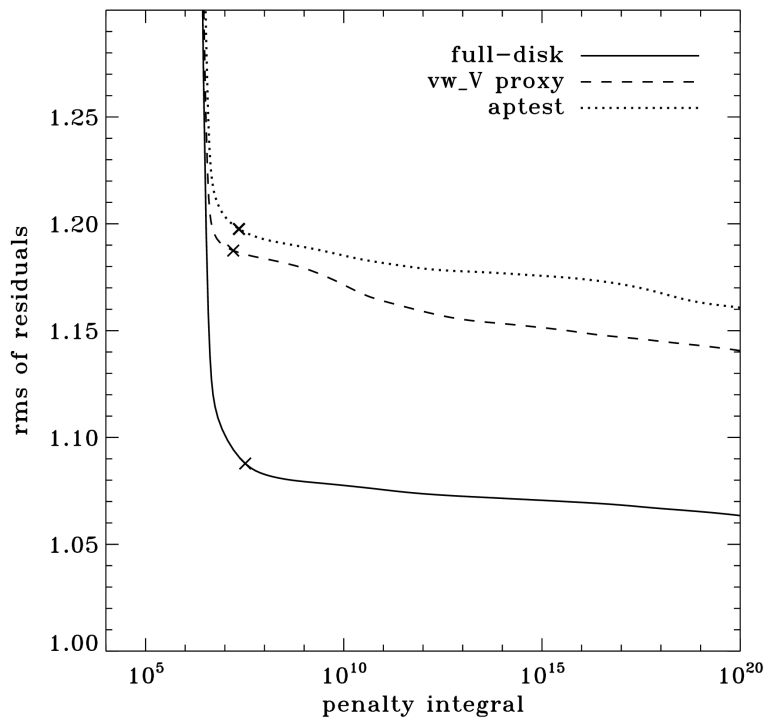
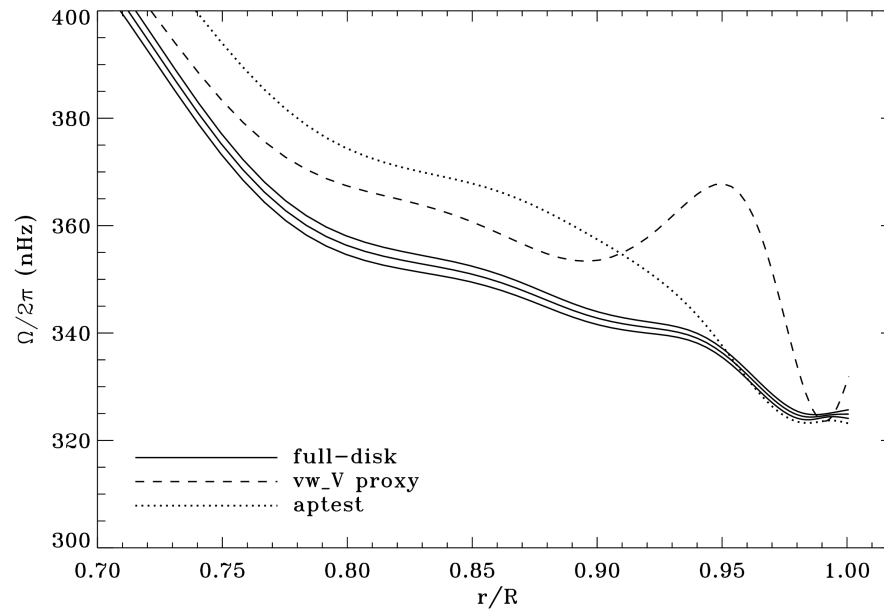
The residuals were marginally increased, and this apodization placed the jet deeper, higher, and wider. As a final test, since the code allows it, we tried an elliptical apodization, compressing by 0.9 in the horizontal direction. This implied a wider (less steep) apodization in the vertical direction.

Low $|B_0|$

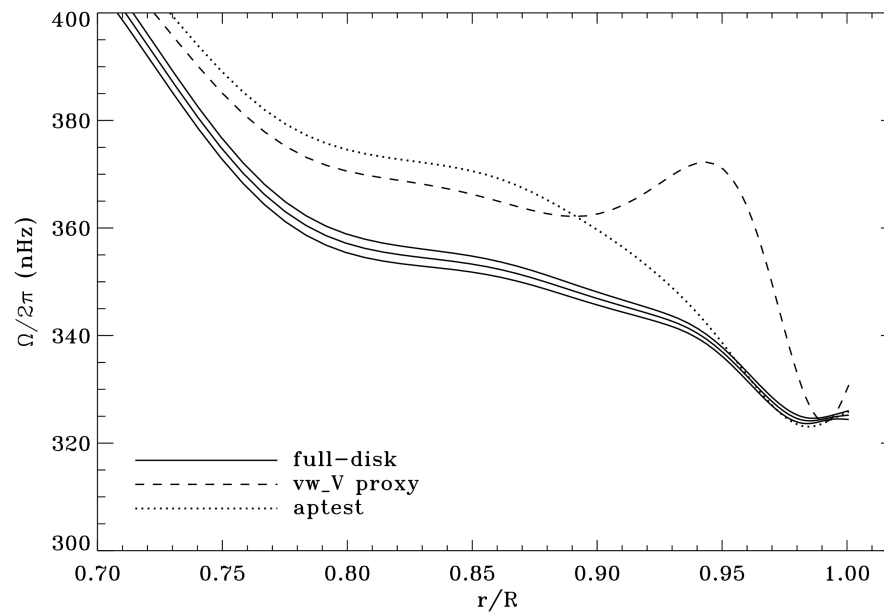




High $|B_0|$



New Leaks



Summary

Using new leaks generally decreased the residuals and the bump for the vw_V data, and improved agreement in the near-surface radial gradient.

Apodizing in longitude/latitude also decreased the residuals and the bump. When using the larger apodizations and a leakage matrix for the actual value of B_0 , the rotation rates did not differ substantially.

Elliptical apodization increased residuals, but improved agreement with full disk near the surface.

Future Work

All inversions presented here used identical tradeoff parameters, but these might be varied for the different analyses.

All mode fitting used leaks up to a maximum Δl of 6, but increasing this might improve the results of the different apodizations.

The effect of the width of the frequency interval used for mode fitting on the results of the different apodizations should be explored.